Statistical State Dynamics of Couette MHD Turbulence

Eojin Kim¹† and Brian F. Farrell¹

¹Department of Earth and Planetary Sciences, Harvard University, Cambridge, MA 02139, USA

(Received xx; revised xx; accepted xx)

The roll streak structure (RSS) is ubiquitous in shear flow turbulence and is fundamental to the dynamics of the self-sustaining process (SSP) maintaining the turbulent state. The formation and maintenance of the RSS in wall-bounded shear flow suggest the presence of an underlying instability that has recently been identified using statistical state dynamics (SSD). Due to the parallelism between the Navier-Stokes equation and the induction equation, it is reasonable to inquire whether the RSS in wall-bounded shear flow has a counterpart in the MHD equations formulated as an SSD. In this work we show that this is the case and that an analytic solution for the composite velocity-magnetic field RSS in the MHD SSD also arises from an instability, that this instability equilibrates to either a fixed point or to a turbulent state, that these turbulent statistical equilibria may be self sustaining, and that both the fixed point and the turbulent states may correspond to large scale coherent dynamos.

1. Introduction

The roll streak structure (RSS) is commonly observed in wall-bounded shear flow turbulence (Kline et al. 1962; Smith & Metzler 1983). The formation of the RSS was originally attributed to the lift-up mechanism (Ellingsen & Palm 1975; Gustavsson 1991). Because the RSS is not unstable in the linearized Navier-Stokes equation (NS) for shear flow it could not be explained as an unstable mode. However, an analytical explanation for its ubiquity in wall bounded shear flow was obtained using optimal perturbation analysis by showing that the RSS is the structure of optimal transient growth (Butler & Farrell 1992; Reddy & Henningson 1993). However, it was subsequently found that the RSS is unstable in turbulent shear flow when the NS is written in statistical state dynamics (SSD) form. This unstable RSS arises by a mechanism in which Reynolds stresses associated with a weakly maintained unstructured background field of turbulence are systematically organized by a perturbation RSS mode to force roll structures properly oriented to maintain the lift-up mechanism underlying the modal instability (Farrell & Ioannou 2012; Farrell et al. 2017). These SSD modal instabilities with RSS form may equilibrate to fixed-point finite-amplitude RSS structures or may, as a function of parameters, transition to chaotic attractor dynamics including self sustaining turbulent states (Farrell & Ioannou 2012).

The omega dynamo growth mechanism in the induction equation is similar to the lift-up process in the NS for shear flow. Therefore, it is reasonable to expect that the omega dynamo mechanism could be similarly destabilized via background turbulence in sheared MHD flow. Because the MHD equations couple the NS and the induction equation, both of which can be expressed separately in SSD form, it is also reasonable to expect that

the MHD equations support nonlinear SSD instabilities, finite state equilibria and RSS turbulence analogous to those previously studied in the context of wall-bounded shear flows. In this work we show that this is the case. The analysis method we use is rooted in the context of generalized stability theory (GST) (Farrell & Ioannou 1996a,b) which has been previously used to study coherent structure formation in the MHD context (Farrell & Ioannou 1999a,b). Specifically, SSD analysis was previously used to study coherent structure dynamics in the context of drift wave turbulence (Farrell & Ioannou 2009b).

Results shown here demonstrate that a combined velocity plus magnetic field RSS is synergistically destabilized by interaction between the NS and the induction equations. The SSD equations used are the MHD equations closed at second order and these equations incorporate the nonlinear mechanisms responsible for equilibrating the unstable RSS modes obtained by perturbation analysis allowing explicit solution for finite amplitude equilibrium states proceeding from these instabilities, both fixed point and turbulent. We find that both the RSS instabilities, the finite amplitude fixed points, and the turbulent solutions may correspond to the emergence of large scale coherent magnetic fields.

Traditional alpha-omega theory destabilizes an omega dynamo using a parameterization to rotate a portion of the toroidal field into poloidal field. In this work, we identify explicitly the dynamics of our equivalent α -effect and the mechanism by which it arises.

In summary, we use the SSD form of the MHD equations to obtain an analytic solution for the composite velocity-magnetic field RSS, show that it arises from an instability, that this instability equilibrates to either a fixed point or to a turbulent state, and show that these states can correspond to large scale coherent dynamos.

2. Governing equations and boundary conditions

We study the dynamics of a turbulent conducting Couette flow with coordinates x, y, z in the streamwise, cross-stream, and spanwise directions, respectively. The governing equations are:

$$\left(\frac{\partial}{\partial t} + \boldsymbol{u} \cdot \nabla\right) \boldsymbol{u} = -\frac{1}{\rho_o} \nabla p + \frac{1}{4\pi \rho_o \mu_o} (\boldsymbol{B} \cdot \nabla) \boldsymbol{B} + \nu \Delta \boldsymbol{u}$$
 (2.1)

$$\frac{\partial \mathbf{B}}{\partial t} + (\mathbf{u} \cdot \nabla) \mathbf{B} = (\mathbf{B} \cdot \nabla) \mathbf{u} + \eta \Delta \mathbf{B}$$
 (2.2)

in which appears the fluid density, ρ_0 , the kinematic viscosity, ν , and the magnetic diffusivity, $\eta = \frac{1}{\mu_o \sigma}$ with μ_0 the permeability and σ the conductivity. Couette channel flow is assumed with distance nondimensionalized by the half cross-stream channel width, L, and velocity by the cross-stream boundary velocity, U. The dimensionless equations are:

$$\left(\frac{\partial}{\partial t} + \boldsymbol{u} \cdot \nabla\right) \boldsymbol{u} = -\nabla p + (\boldsymbol{B} \cdot \nabla) \boldsymbol{B} + \frac{1}{Re} \Delta \boldsymbol{u}$$
(2.3)

$$\frac{\partial \boldsymbol{B}}{\partial t} + (\boldsymbol{u} \cdot \nabla) \boldsymbol{B} = (\boldsymbol{B} \cdot \nabla) \boldsymbol{u} + \frac{1}{Re_m} \boldsymbol{B}$$
 (2.4)

in which appear the Reynolds number and magnetic Reynolds number defined in terms

of the kinematic viscosity, ν , and the magnetic diffusivity, η :

$$Re = \frac{UL}{\nu}, \quad Re_m = \frac{UL}{n}.$$
 (2.5)

Periodic boundary conditions are imposed in the streamwise and spanwise directions and impenetrable no-slip for the velocity field and vanishing of the magnetic field at the the cross-steam boundaries.

$$\mathbf{u}(y=1) = 1\hat{i}, \mathbf{B}(y=1) = 0 \tag{2.6}$$

$$\mathbf{u}(y = -1) = -1\hat{i}, \mathbf{B}(y = -1) = 0 \tag{2.7}$$

3. Formulation of MHD turbulence as a SSD

Our focus is on studying composite velocity-magnetic field RSS dynamics using the MHD equations in SSD form. The choice of Reynolds average is crucial in constructing an SSD that represents the underlying physics in the most transparent manner. We choose the streamwise average for our Reynolds average and use an overbar to denote an averaged variable so that:

$$\overline{\boldsymbol{u}} = [\boldsymbol{u}]_x = \overline{u}_x(y, z, t)\hat{i} + \overline{u}_y(y, z, t)\hat{j} + \overline{u}_z(y, z, t)\hat{k}$$
(3.1)

$$\overline{\boldsymbol{B}} = [\boldsymbol{B}]_x = \overline{B}_x(y, z, t)\hat{i} + \overline{B}_y(y, z, t)\hat{j} + \overline{B}_z(y, z, t)\hat{k}. \tag{3.2}$$

We decompose state variables into streamwise mean and fluctuations:

$$\boldsymbol{u}(x,y,z,t) = \overline{\boldsymbol{u}}(y,z,t) + \boldsymbol{u'}(x,y,z,t) \tag{3.3}$$

$$\boldsymbol{B}(x,y,z,t) = \overline{\boldsymbol{B}}(y,z,t) + \boldsymbol{B'}(x,y,z,t). \tag{3.4}$$

The equations for the streamwise means are:

$$\frac{\partial \overline{u}}{\partial t} = -(\overline{u} \cdot \nabla)\overline{u} - \overline{u'} \cdot \nabla \overline{u'} - \nabla P + (\overline{B} \cdot \nabla)\overline{B} + \overline{(B'} \cdot \nabla)\overline{B'} + \frac{1}{R_e} \Delta \overline{u}$$
(3.5)

$$\frac{\partial \overline{B}}{\partial t} = -(\overline{u} \cdot \nabla) \overline{B} + (\overline{B} \cdot \nabla) \overline{u} - \overline{(u' \cdot \nabla) B'} + (\overline{B' \cdot \nabla) u'} + \frac{1}{Re_m} \Delta \overline{B}.$$
 (3.6)

The fluctuation equations result from subtracting the mean equations from the full equations:

$$\frac{\partial \boldsymbol{u'}}{\partial t} = -(\overline{\boldsymbol{u}} \cdot \nabla) \boldsymbol{u'} - (\boldsymbol{u'} \cdot \nabla) \overline{\boldsymbol{u}} - \nabla p' + (\overline{\boldsymbol{B}} \cdot \nabla) \boldsymbol{B'} + (\boldsymbol{B'} \cdot \nabla) \overline{\boldsymbol{B}} + \frac{1}{Re} \Delta \boldsymbol{u'} + \epsilon_{\boldsymbol{u'}\boldsymbol{u'}}^{1/2} F_{\boldsymbol{u'}} \boldsymbol{\xi}(\boldsymbol{t}) \quad (3.7)$$

$$\frac{\partial \mathbf{B'}}{\partial t} = -(\overline{\mathbf{u}} \cdot \nabla) \mathbf{B'} - (\mathbf{u'} \cdot \nabla) \overline{\mathbf{B}} + (\overline{\mathbf{B}} \cdot \nabla) \mathbf{u'} + (\mathbf{B'} \cdot \nabla) \overline{\mathbf{u}} + \frac{1}{Re_m} \Delta \mathbf{B'} + \epsilon_{\mathbf{B'B'}}^{1/2} \mathbf{F_{B'}} \mathbf{\chi}(t) \quad (3.8)$$

in which a stochastic parameterization formed by the fluctuation structure matrices $F_{u'}$, $F_{B'}$ and vectors of independent temporally delta-correlated stochastic processes $\xi(t)$, $\chi(t)$ replaces the non-linear fluctuation-fluctuation interaction terms in the momentum and induction equations (3.7), (3.8). These stochastic terms also serve to parameterize any exogenous excitation in the model. Note that with this parameterization for the nonlinear terms in the fluctuation equations, the fluctuation equations become linear and the resulting overall dynamics is quasi-linear.

We define the mean state variable as

$$\Gamma = [\overline{u}, \overline{B}]^T. \tag{3.9}$$

The mean equation can be written as:

$$\frac{\partial \boldsymbol{\Gamma}}{\partial t} = \begin{bmatrix} -(\overline{\boldsymbol{u}} \cdot \nabla)\overline{\boldsymbol{u}} - \nabla P + (\overline{\boldsymbol{B}} \cdot \nabla)\overline{\boldsymbol{B}} + \frac{1}{Re}\Delta\overline{\boldsymbol{u}} \\ -(\overline{\boldsymbol{u}} \cdot \nabla)\overline{\boldsymbol{B}} + (\overline{\boldsymbol{B}} \cdot \nabla)\overline{\boldsymbol{u}} + \frac{1}{Re_{\eta}}\Delta\overline{\boldsymbol{B}} \end{bmatrix} + \begin{bmatrix} -(\overline{\boldsymbol{u'} \cdot \nabla})\boldsymbol{u'} + \overline{(\boldsymbol{B'} \cdot \nabla)\boldsymbol{B'}} \\ -(\overline{\boldsymbol{u'} \cdot \nabla})\boldsymbol{B'} + (\overline{\boldsymbol{B'} \cdot \nabla})\boldsymbol{u'} \end{bmatrix}$$
(3.10)

We define the fluctuation state variable as:

$$\phi \equiv [\mathbf{u'}, \mathbf{B'}]^T. \tag{3.11}$$

To formulate a SSD closed at second order, an equation for the infinite ensemble average fluctuation covariance $C \equiv \langle \phi \phi^T \rangle$ is required. Under the assumption that the stochastic closure is white in time, an evolution equation for the infinite ensemble average covariance of the fluctuation state can be obtained in the form of a time dependent Lyapunov equation (Farrell & Ioannou 2019):

$$\partial_t \mathbf{C} = \mathbf{A}(\mathbf{\Gamma})\mathbf{C} + \mathbf{C}\mathbf{A}(\mathbf{\Gamma})^{\dagger} + \mathbf{Q} \tag{3.12}$$

in which A is the linear operator of the fluctuation equations (3.7) and (3.8) and the stochastic closure is

$$Q = \begin{bmatrix} \epsilon_{u'u'} Q_{u'u'} & 0\\ 0 & \epsilon_{B'B'} Q_{B'B'} \end{bmatrix}$$
(3.13)

in which the fluctuation excitation structure correlation matrices appear:

$$Q_{u'u'} = F_{u'}F_{u'}^{\dagger} \tag{3.14}$$

$$Q_{B'B'} = F_{B'}F_{B'}^{\dagger}. \tag{3.15}$$

The spatial covariance of the excitation structures, $Q_{u'u'}$ and $Q_{B'B'}$, are chosen to excite each degree of freedom equally in energy which is accomplished by choosing Q to

be the identity.

We refer to this second order SSD as the S3T SSD and write it in compact form as:

$$\partial_t \Gamma = G(\Gamma) + L_{RS}C \tag{3.16}$$

$$\partial_t \mathbf{C} = \mathbf{A}(\mathbf{\Gamma})\mathbf{C} + \mathbf{C}\mathbf{A}(\mathbf{\Gamma})^{\dagger} + \mathbf{Q} \tag{3.17}$$

where

$$G(\Gamma) = \begin{bmatrix} -(\overline{u} \cdot \nabla)\overline{u} - \nabla P + (\overline{B} \cdot \nabla)\overline{B} + \frac{1}{Re}\Delta\overline{u} \\ -(\overline{u} \cdot \nabla)\overline{B} + (\overline{B} \cdot \nabla)\overline{u} + \frac{1}{Re_m}\Delta\overline{B} \end{bmatrix}$$
(3.18)

$$L_{RS}C = \begin{bmatrix} -(\overline{u' \cdot \nabla})\overline{u'} + (\overline{B' \cdot \nabla})\overline{B'} \\ -(\overline{u' \cdot \nabla})\overline{B'} + (\overline{B' \cdot \nabla})\overline{u'} \end{bmatrix}.$$
 (3.19)

$$Q = \begin{bmatrix} \epsilon_{u'u'} Q_{u'u'} & 0\\ 0 & \epsilon_{B'B'} Q_{B'B'} \end{bmatrix}$$
(3.20)

For the purpose of integration and to isolate as diagnostic variables the streamwise mean streamwise velocity and magnetic field components and the streamwise mean spanwise-cross stream velocity and magnetic field we take advantage of the velocity and magnetic fields being nondivergent to write the S3T SSD mean equations using as state variables for the streamwise mean state the streamwise component of velocity and of magnetic field and the cross-stream-spanwise components of velocity and magnetic field expressed using streamfunctions as $\Gamma = [\overline{u}_x, \Psi, \overline{B}_x, \Xi]^T$ with the mean velocity and magnetic field streamfunctions respectively defined as:

$$-\partial_z \Psi = \overline{u_y}, \quad \partial_y \Psi = \overline{u_z} \tag{3.21}$$

$$-\partial_z \Xi = \overline{B_y}, \quad \partial_y \Xi = \overline{B_z}. \tag{3.22}$$

The mean state dynamics exclusive of the fluctuation-fluctuation term are:

$$G(\Gamma) = \begin{bmatrix} G_{\overline{u}_x}(\Gamma) \\ G_{\Psi}(\Gamma) \\ G_{\overline{B}_x}(\Gamma) \\ G_{\Xi}(\Gamma) \end{bmatrix}, \tag{3.23}$$

in which are defined separately the equations for the mean components of the velocity and magnetic field:

$$G_{\overline{u}_x}(\mathbf{\Gamma}) = \partial_y \overline{u_x} \partial_z \Psi - \partial_z \overline{u_x} \partial_y \Psi + \Delta_1 \frac{\overline{u_x}}{Re} - \partial_y \overline{B_x} \partial_z \Xi + \partial_z \overline{B_x} \partial_y \Xi + \frac{1}{Re} \Delta \overline{u}_x \qquad (3.24)$$

$$G_{\Psi}(\mathbf{\Gamma}) = \Delta^{-1}[(\partial_{yy} - \partial_{zz})(\partial_{y}\Psi \partial_{z}\Psi - \partial_{y}\Xi \partial_{z}\Xi) - \partial_{yz}((\partial_{y}\Psi)^{2} - (\partial_{z}\Psi)^{2} - (\partial_{y}\Xi)^{2} + (\partial_{z}\Xi)^{2}) + \frac{1}{Re}\Delta\Delta\overline{\Psi}]$$

$$(3.25)$$

$$G_{\overline{B}_x}(\mathbf{\Gamma}) = \frac{\partial(-\overline{u_x}\partial_z \Xi + \partial_z \Psi \overline{B_x})}{\partial y} - \frac{\partial(\partial_y \Psi \overline{B_x} - \overline{u_x}\partial_y \Xi)}{\partial z} + \frac{1}{Re_m} \Delta \overline{B}_x$$
(3.26)

$$G_{\Xi}(\mathbf{\Gamma}) = \Delta^{-1} \left[-(\partial_{yy} + \partial_{zz})(-\partial_z \Psi \partial_y \Xi + \partial_y \Psi \partial_z \Xi) + \frac{1}{Re_m} \Delta \Delta \Xi \right]$$
(3.27)

The fluctuation-fluctuation term in the mean equation is:

$$L_{RS}C = \begin{bmatrix} -\partial_{y}\overline{u'_{x}u'_{y}} - \partial_{z}\overline{u'_{x}u'_{z}} + \partial_{y}\overline{B'_{x}B'_{y}} + \partial_{z}\overline{B'_{x}B'_{z}} \\ \Delta^{-1}[(\partial_{yy} - \partial_{zz})(-\overline{u'_{y}u'_{z}} + \overline{B'_{y}B'_{z}}) - \partial_{yz}(u'_{z}^{'2} - \overline{u'_{y}^{'2}} - \overline{B'_{z}^{'2}} + \overline{B'_{y}^{'2}})] \\ + \frac{\partial(\overline{u'_{x}B'_{y}} - u'_{y}B'_{x}}{\partial y} - \frac{\partial(\overline{u'_{z}B'_{x}} - u'_{x}B'_{z})}{\partial z} \\ \Delta^{-1}[-(\partial_{yy} + \partial_{zz})(\overline{u'_{y}B'_{z}} - \overline{u'_{z}B'_{y}})] \end{bmatrix}$$
(3.28)

In a similar manner, for the purpose of integration the fluctuation covariance equation (3.17) is written in terms of cross stream components of velocity and magnetic field and cross stream components of curl of velocity and of magnetic field. To this end, the fluctuation state variable is written as $\phi = [u'_y, \omega'_y, B'_y, \zeta'_y]^T$ with the velocity and magnetic curl quantities:

$$\omega_y' = \partial_z u_x' - \partial_x u_z' \tag{3.29}$$

$$\zeta_y' = \partial_z B_x' - \partial_x B_z'. \tag{3.30}$$

The ensemble average fluctuation covariance $C \equiv \langle \phi \phi^T \rangle$ is expressed using these variables and both $Q_{u'u'}$ and $Q_{B'B'}$ are consistently transformed (Kim & Farrell 2025; Farrell & Ioannou 2012). The Lyapunov equation (3.17) is then integrated in these variables.

4. S3T stability formulation

Assuming an equilibrium S3T state, (Γ_e, C_e) , in which the LHS of (3.16) and (3.17) vanish:

$$\boldsymbol{\varGamma}_{e} = \begin{bmatrix} \overline{u}_{xe} \\ \underline{\Psi}_{e} \\ \overline{B}_{xe} \\ \underline{\Xi}_{e} \end{bmatrix} \tag{4.1}$$

and following (Farrell & Ioannou 2012, 2019; Farrell et al. 2017) perturbation equations linearized around the SSD equilibrium state (Γ_e , C_e) can be obtained:

$$\partial_t(\delta \mathbf{\Gamma}) = \sum_i \frac{\partial \mathbf{G}}{\partial \Gamma_i} |_{\Gamma_e} \delta \Gamma_i + \mathbf{L}_{RS} \delta \mathbf{C}$$
(4.2)

$$\partial_t(\delta \mathbf{C}) = \mathbf{A}_e \delta \mathbf{C} + \delta \mathbf{C} \mathbf{A}_e^{\dagger} + \delta \mathbf{A} \mathbf{C}_e + \mathbf{C}_e \delta \mathbf{A}^{\dagger}$$
(4.3)

where

$$\delta \mathbf{A} = \mathbf{A}(\mathbf{\Gamma}_e + \delta \mathbf{\Gamma}) - \mathbf{A}(\mathbf{\Gamma}_e). \tag{4.4}$$

Equations (4.2) and (4.3) comprise the formulation of the linear perturbation S3T dynamics.

5. Stability analysis of the composite velocity and magnetic field RSS in the S3T SSD of turbulent Couette flow

In this section, we focus on the linear stability of (4.2) - (4.3). While in non-conducting Couette flow the S3T SSD supports velocity state only instabilities with RSS structure (Farrell & Ioannou 2012; Farrell *et al.* 2017), we find that both the velocity field and the magnetic field participate synergistically in destabilizing the RSS in turbulent conducting Couette flow.

We use Fourier series to represent fluctuations in the streamwise direction, x, and the spanwise direction, z. The channel domain size in x and z are $Lx=1.75\pi$ and $Lz=1.2\pi$, respectively. A single streamwise wavenumber and 8 spanwise wavenumbers are retained in x and z along with Ny=25 grid points in y. Retaining a single wavenumber in x is consistent with self-sustaining turbulence in our model being supported solely by this wavenumber (Farrell & Ioannou 2012). For convenience, $Q_{u'u'}$ and $Q_{B'B'}$ are replaced by $Q_{u'u'}$ and $Q_{B'B'}$ such that $\epsilon_{u'u'}=1$ and $\epsilon_{B'B'}=1$ results in volume averaged RMS fluctuation velocity and magnetic field being 1 % of the maximum velocity of the Couette profile. Explicitly, $[\sqrt{u'_x^2+u'_y^2+u'_z^2}]_{y,z}=0.01$ and $[\sqrt{B'_x^2+B'_y^2+B'_z^2}]_{y,z}=0.01$. Results are presented for $Re=Re_m=400$.

The stability diagram for turbulence excitation parameters $\epsilon_{u',u'}$ and $\epsilon_{B',B'}$ is shown in panel a of figure 1. Panel b and c of this figure show the velocity field structure $\delta \overline{u}$ and magnetic field structure $\delta \overline{B}$ of the unstable eigenmode at parameter values $\epsilon_{u',u'}=4$ and $\epsilon_{B',B'}=5$ (indicated by a star in panel (a) of figure 1). Noteworthy are that the velocity and magnetic field components of the RSS are generally similar in structure despite the physically distinct mechanisms involved in the NS and induction equations. The amplitude of the fields being similar indicates approximate energy equipartition in view of the scaling used for the velocity and magnetic fields. The characteristic 90 degree phase shift between the $\delta \overline{u}$ and $\delta \overline{B}$ fields indicates a synergy operating between these fields in maintaining their composite structure.

6. Equilibration of RSS instabilities in the S3T SSD

The S3T SSD is a nonlinear system with an equilibration mechanism consistent with its underlying MHD dynamics. Perturbing the Couette S3T SSD model with unstable

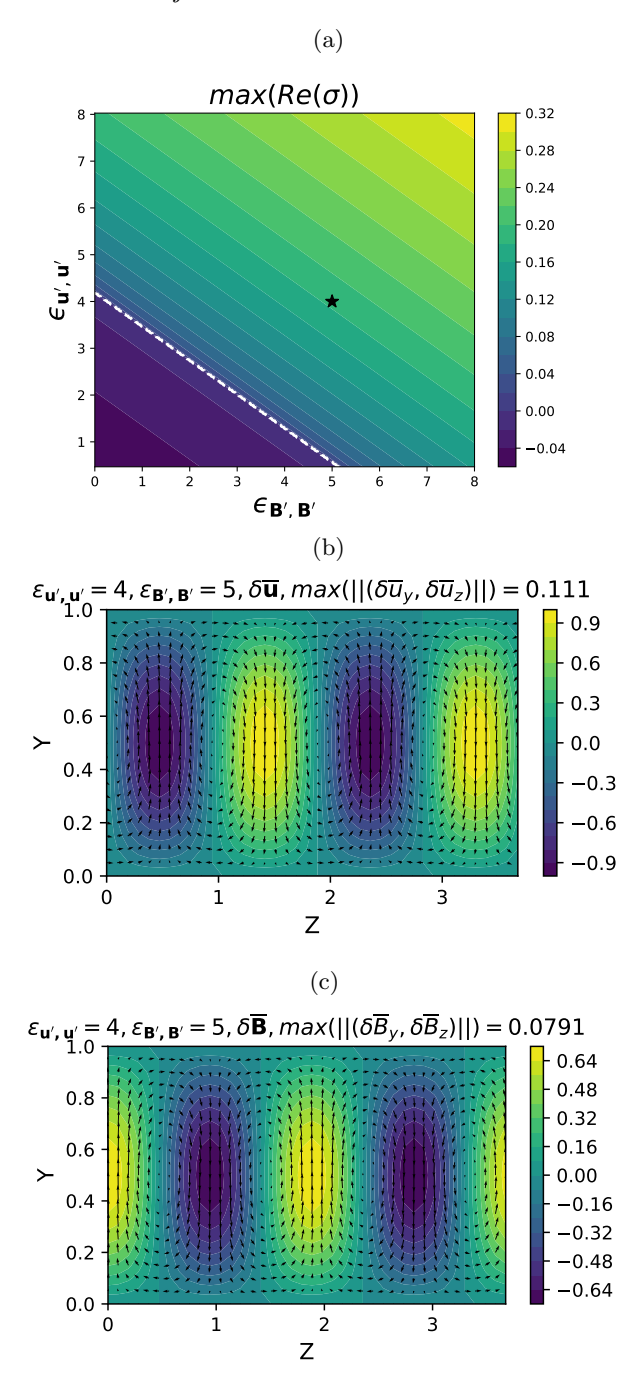


Figure 1: Panel(a): stability diagram for turbulence excitation parameters $\epsilon_{u',u'}$ and $\epsilon_{B',B'}$. Panel (b): streamwise velocity contours and spanwise/cross-stream velocity vectors of most unstable eigenmode. Panel (c): streamwise magnetic field contours and spanwise/cross-stream magnetic field vectors of most unstable eigenmode. Eigenfunction structures have been normalized so that the maximum value of $\delta \overline{u}_x$ is unity. The location of the unstable mode at $\epsilon_{u',u'} = 4$ and $\epsilon_{B',B'} = 5$ is indicated with a star in panel (a).

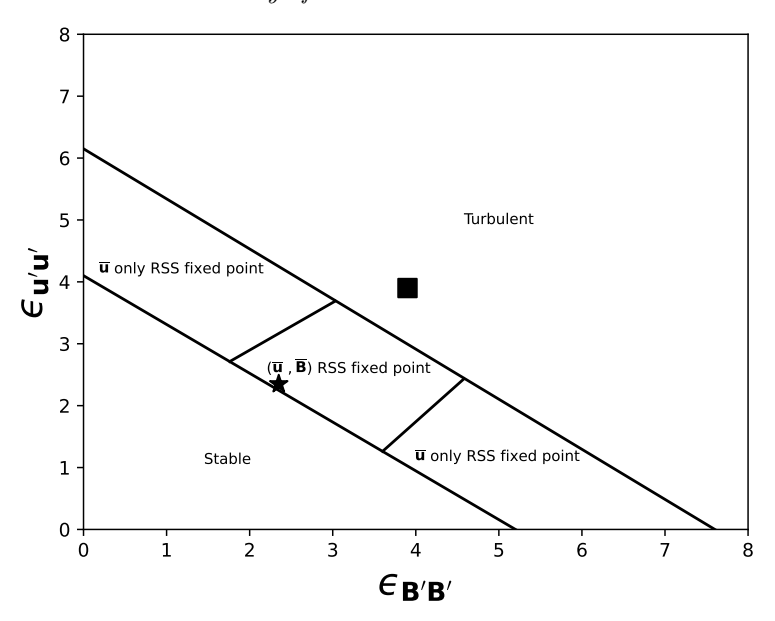


Figure 2: Equilibrium regime diagram for turbulence excitation parameters $\epsilon_{u',u'}$, $\epsilon_{B',B'}$ for $Re = Re_m = 400$

RSS eigenmodes results in establishing a finite-amplitude equilibrium consisting of a fixed point RSS, or transition to a time-dependent or turbulent state depending on parameter values. As a summary of our findings and to set the stage for presenting our results, an equilibrium structure diagram as a function of $\epsilon_{u'u'}$ and $\epsilon_{B'B'}$ is shown in figure 2. We turn now to examine salient aspects of these equilibrium regimes.

Unlike analogous regime diagrams for nonconducting wall bounded shear flow (Farrell et al. 2017), figure 2 contains two distinct fixed point regimes: a fixed point regime supporting an RSS with only a coherent mean velocity, \overline{u} , component and a fixed point regime supporting an RSS in which both a coherent mean velocity, \overline{u} , and a coherent mean magnetic field, \overline{B} , are maintained. In figure 3 is shown the RSS structure of a fixed point equilibrium at $\epsilon_{u'u'} = 2.35$ and $\epsilon_{B'B'} = 2.35$ (marked by a star in figure 2) in which both a coherent velocity field and a coherent magnetic field are supported. In this fixed-point equilibrium RSS both the roll velocity field and the poloidal magnetic field components of the RSS, along with the 90 degree phase relation between these components, agree with the structure of the S3T perturbation instability for these parameters as shown in figure 1. We conclude that the unstable RSS mode qualitatively predicts the equilibrium structure of the finite amplitude equilibrium. As shown in figure 2 above, a region of parameter space exists with fixed point equilibria in which the RSS maintains finite amplitude components in both the roll and streak velocity and the poloidal and toroidal magnetic field. However, when the difference between the velocity and magnetic turbulence excitations, $|\epsilon_{u'u'} - \epsilon_{B'B'}|$, becomes sufficiently large, the fixed point RSS supports only a coherent velocity field component, \overline{u} .

While a too great difference in velocity turbulence excitation, $\epsilon_{\boldsymbol{u'u'}}$, and magnetic turbulence excitation, $\epsilon_{\boldsymbol{B'B'}}$, leads to suppression of the magnetic field component of the fixed point equilibrium, coherent large scale RSS structures in both magnetic field and velocity field are supported by background turbulence excitation once the transition to turbulence occurs, even when the difference between the amplitudes, $|\epsilon_{\boldsymbol{u'u'}} - \epsilon_{\boldsymbol{B'B'}}|$, is

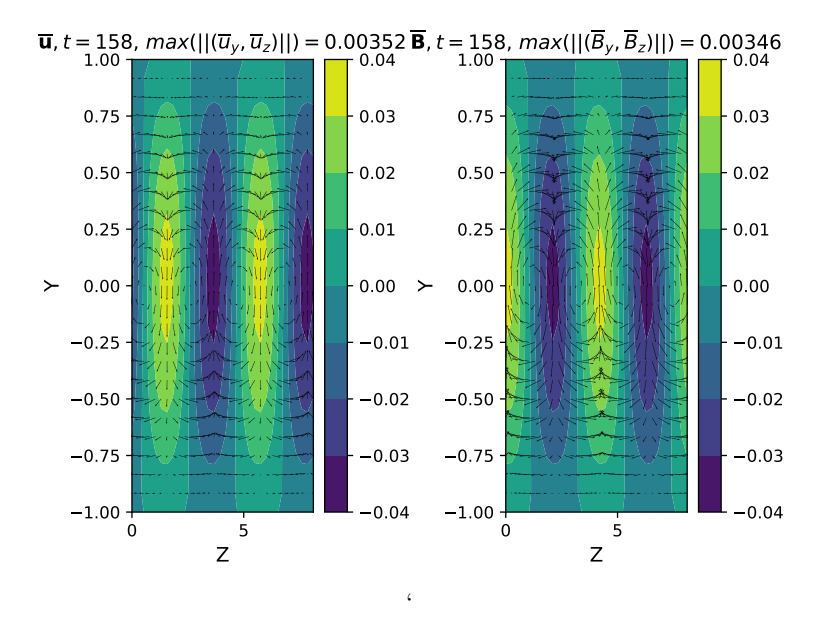


Figure 3: Fixed point equilibrium RSS supporting finite amplitude components in both the mean velocity field \overline{u} and the mean magnetic field \overline{B} . On the left: streak velocity $\overline{u}_{xs} = \overline{u}_x - [\overline{u}_x]_z$ (contours) and roll velocity $(\overline{u}_y, \overline{u}_z)$ (vectors). On the right: streak magnetic field $\overline{B}_{xs} = \overline{B}_x - [\overline{B}_x]_z$ (contours) and roll magnetic field $(\overline{B}_y, \overline{B}_z)$ (vectors). Parameters: $\epsilon_{u'u'} = 2.35$ and $\epsilon_{B'B'} = 2.35$, $Re = Re_m = 400$

large. Snapshots of turbulent equilibria at $\epsilon_{u'u'} = 3.9$ and $\epsilon_{B'B'} = 3.9$ (marked by a square in figure 2) are shown in figure 4.

7. Self sustaining RSS turbulence

In wall-bounded hydrodynamic turbulence a turbulent RSS state can self sustain with $\epsilon_{\boldsymbol{u'u'}} = 0$ once it has transitioned to turbulence (Farrell & Ioannou 2012). It is of interest to inquire whether the turbulent MHD RSS can sustain without the presence of $\epsilon_{\boldsymbol{u'u'}}$ and $\epsilon_{\boldsymbol{B'B'}}$. To address this question we excite a turbulent RSS state using $\epsilon_{\boldsymbol{u'u'}}$ and $\epsilon_{\boldsymbol{B'B'}}$ and then turn off support for $\epsilon_{\boldsymbol{u'u'}}$ and $\epsilon_{\boldsymbol{B'B'}}$ as a diagnostic for the existence of a self sustaining turbulent state.

More explicitly, after developing fully turbulent states, $\epsilon_{u'u'}$ and $\epsilon_{B'B'}$ are set to zero resulting in the following equations:

$$\partial_t \mathbf{\Gamma} = \mathbf{G}(\mathbf{\Gamma}) + \mathbf{L}_{RS} \mathbf{C} \tag{7.1}$$

$$\partial_t C = A(\Gamma)C + CA(\Gamma)^{\dagger}. \tag{7.2}$$

Shown in figure 5 is the result of eliminating the excitation in our example case at $Re = 400, Pr_m = 1$ (corresponding to a star in figure 6) showing that only the velocity self sustains while the magnetic field decays. At a given Re, existence of a SSP supporting both a coherent velocity and a coherent magnetic field component in the RSS depends on magnetic Prandtl number:

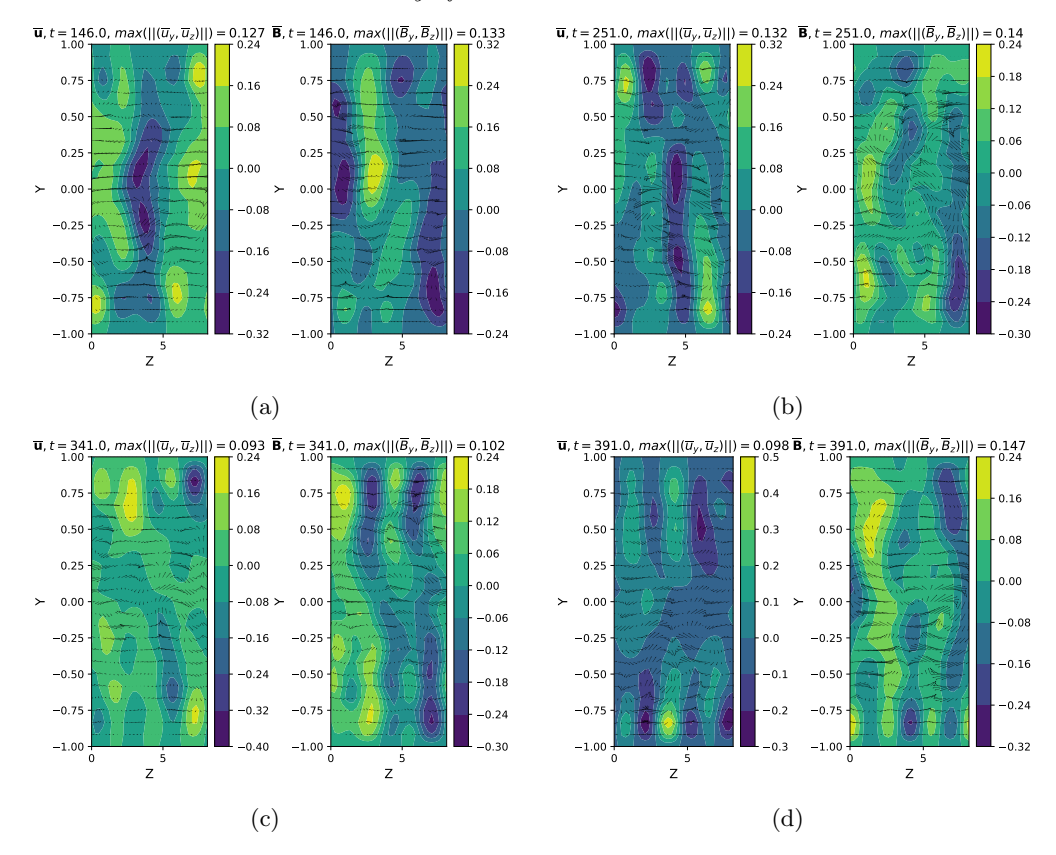


Figure 4: Snapshots of turbulent equilibria supporting finite amplitude components in both the mean velocity field $\overline{\boldsymbol{u}}$ and the mean magnetic field $\overline{\boldsymbol{B}}$. For each snapshot, on the left: streak velocity $\overline{u}_{xs} = \overline{u}_x - [\overline{u}_x]_z$ (contours) and roll velocity $(\overline{u}_y, \overline{u}_z)$ (vectors). On the right: streak magnetic field $\overline{B}_{xs} = \overline{B}_x - [\overline{B}_x]_z$ (contours) and roll magnetic field $(\overline{B}_y, \overline{B}_z)$ (vectors). Parameters: $\epsilon_{\boldsymbol{u}'\boldsymbol{u}'} = 3.9$ and $\epsilon_{\boldsymbol{B}'\boldsymbol{B}'} = 3.9$, $Re = Re_m = 400$

$$Pr_m = \frac{\eta}{\mu} = \frac{Re_m}{Re}. (7.3)$$

To demonstrate this, we show in figure 6 the time averaged value of magnetic streak energy:

$$E_{\overline{B}_{xs}} \equiv \frac{1}{2} [\overline{B}_{xs}^2]_{y,z}, \tag{7.4}$$

which is diagnostic of the existence of a coherent magnetic field component, as a function of Pr_m . Bifurcation from a self sustaining state in the velocity field only to a self sustaining state in both the velocity and the magnetic field, which is indicative of a dynamo, is seen in figure 6 to occur at critical magnetic Prandtl number $Pr_{mc} \approx 1.22$.

Consistent with this result, at Re = 400, $Pr_m = 1.5$ (marked by a square in figure 6), a self sustaining turbulent RSS is maintained that supports both a coherent mean

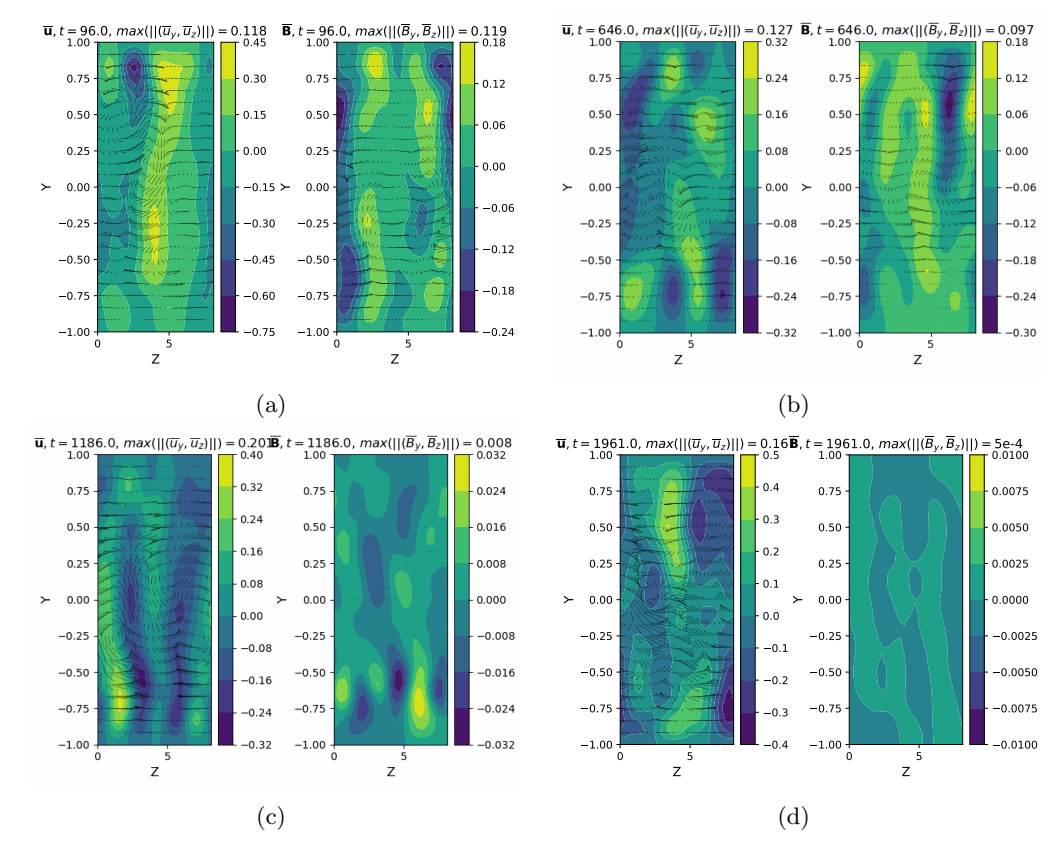


Figure 5: Snapshots of self sustaining turbulent equilibria sustaining finite amplitude components in only the mean velocity \overline{u} . For each snapshot, on the left: streak velocity $\overline{u}_{xs} = \overline{u}_x - [\overline{u}_x]_z$ (contours) and roll velocity $(\overline{u}_y, \overline{u}_z)$ (vectors). On the right: streak magnetic field $\overline{B}_{xs} = \overline{B}_x - [\overline{B}_x]_z$ (contours) and roll magnetic field $(\overline{B}_y, \overline{B}_z)$ (vectors). Parameters: $Re = Re_m = 400$, $\epsilon_{u'u'} = \epsilon_{B'B'} = 0$

velocity and magnetic field component. Snapshots of this self sustaining state are shown in figure 7.

It's also important to point out that while we obtained $Pr_{mc} \approx 1.22 > 1$ for Re = 400, Pr_{mc} is a function of Reynolds number and Pr_{mc} isn't necessarily greater than unity. For example, at Re = 600, $Pr_{mc} \approx 0.83 < 1$, which shows that self sustaining dynamos can exist in our system at both $Pr_m > 1$ and $Pr_m < 1$.

8. Mechanisms maintaining the velocity component in turbulent MHD RSS

We now consider the physical mechanisms maintaining the RSS in turbulent MHD Couette flow and relate these to the mechanisms maintaining the RSS in wall-bounded shear flows. Unlike the case of the RSS in wall bounded shear flows, in MHD Couette turbulence the RSS is a composite structure consisting of interacting components in both the velocity \overline{u} and the magnetic field \overline{B} . We begin by extending previous studies on velocity field RSS maintenance in wall bounded shear flow turbulence (Farrell et al. 2016) to the MHD case. In that study the mechanisms underlying RSS dynamics

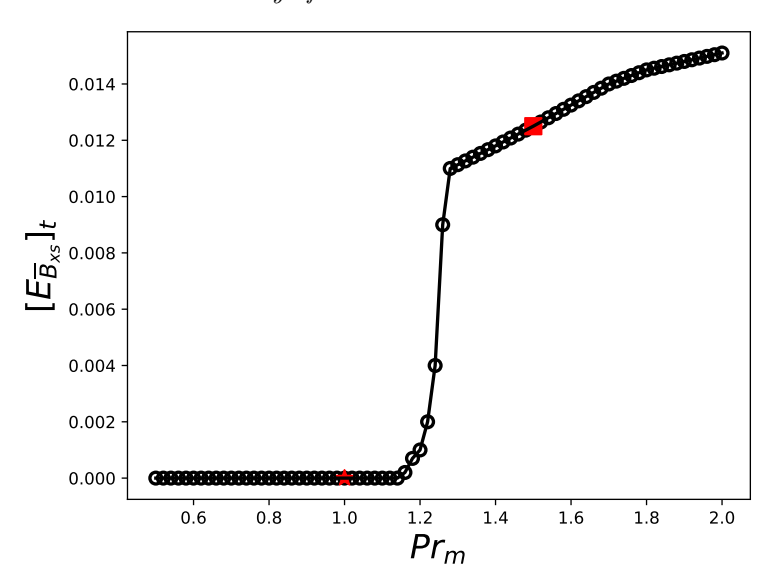


Figure 6: Magnetic streak energy diagostic for a self sustaining state in the magnetic field component of the RSS as a function of Prandtl number, Pr_m

and equilibration were examined using balance equations for the RSS streak velocity, $\overline{u}_{xs} \equiv \overline{u}_x - [\overline{u}_x]_z$, and roll vorticity, $\overline{\omega}_{xr} \equiv \overline{\omega}_x - [\overline{\omega}_x]_z$, where the streamwise component of vorticity is defined as $\overline{\omega}_x = -\partial_z \overline{u}_y + \partial_y \overline{u}_z$.

We first study maintenance of the streak velocity component of the RSS, \overline{u}_{xs} , for which the balance equation is:

$$\partial_{t}\overline{u}_{xs} = -(\overline{u}_{y}\frac{\partial\overline{u}_{x}}{\partial y} - [\overline{u}_{y}\frac{\partial\overline{u}_{x}}{\partial y}]_{z}) - (\overline{u}_{z}\frac{\partial\overline{u}_{x}}{\partial z} - [\overline{u}_{z}\frac{\partial\overline{u}_{x}}{\partial z}]_{z})$$

$$-([u'_{y}\frac{\partial u'_{x}}{\partial y}]_{x} - [u'_{y}\frac{\partial u'_{x}}{\partial y}]_{x,z}) - ([u'_{z}\frac{\partial u'_{x}}{\partial z}]_{x} - [u'_{z}\frac{\partial u'_{x}}{\partial z}]_{x,z})$$

$$+\frac{\partial\overline{B_{x}B_{y}} - [\overline{B_{x}B_{y}}]_{z}}{\partial y} + \frac{\partial\overline{B_{x}B_{z}}}{\partial z} + \frac{\partial\overline{B'_{x}B'_{y}} - [\overline{B'_{x}B'_{y}}]_{z}}{\partial y} + \frac{\partial\overline{B'_{x}B'_{z}}}{\partial z} + \Delta_{1}\frac{\overline{u}_{xs}}{Re}.$$

$$(8.1)$$

Because streaks of both signs occur, obtaining a linear measure of streak forcing requires multiplying each term by the local $sign(\overline{u}_{xs})$. Equations for physically distinct terms in the dynamics maintaining \overline{u}_{xs} are:

$$I_A = sign(\overline{u}_{xs}) \cdot \left(-\left(\overline{u_y} \frac{\partial \overline{u_x}}{\partial y} - \left[\overline{u_y} \frac{\partial \overline{u_x}}{\partial y}\right]_z \right) - \left(\overline{u_z} \frac{\partial \overline{u_x}}{\partial z} - \left[\overline{u_z} \frac{\partial \overline{u_x}}{\partial z}\right]_z \right) \right)$$
(8.2)

$$I_B = sign(\overline{u}_{xs}) \cdot \left(-\left(\left[u_y' \frac{\partial u_x'}{\partial u} \right]_x - \left[u_y' \frac{\partial u_x'}{\partial u} \right]_{x,z} \right) - \left(\left[u_z' \frac{\partial u_x'}{\partial z} \right]_x - \left[u_z' \frac{\partial u_x'}{\partial z} \right]_{x,z} \right) \right)$$
(8.3)

$$I_C = sign(\overline{u}_{xs}) \cdot \left(\frac{\partial \overline{B_x B_y} - [\overline{B_x B_y}]_z}{\partial y} + \frac{\partial \overline{B_x B_z}}{\partial z}\right)$$
(8.4)

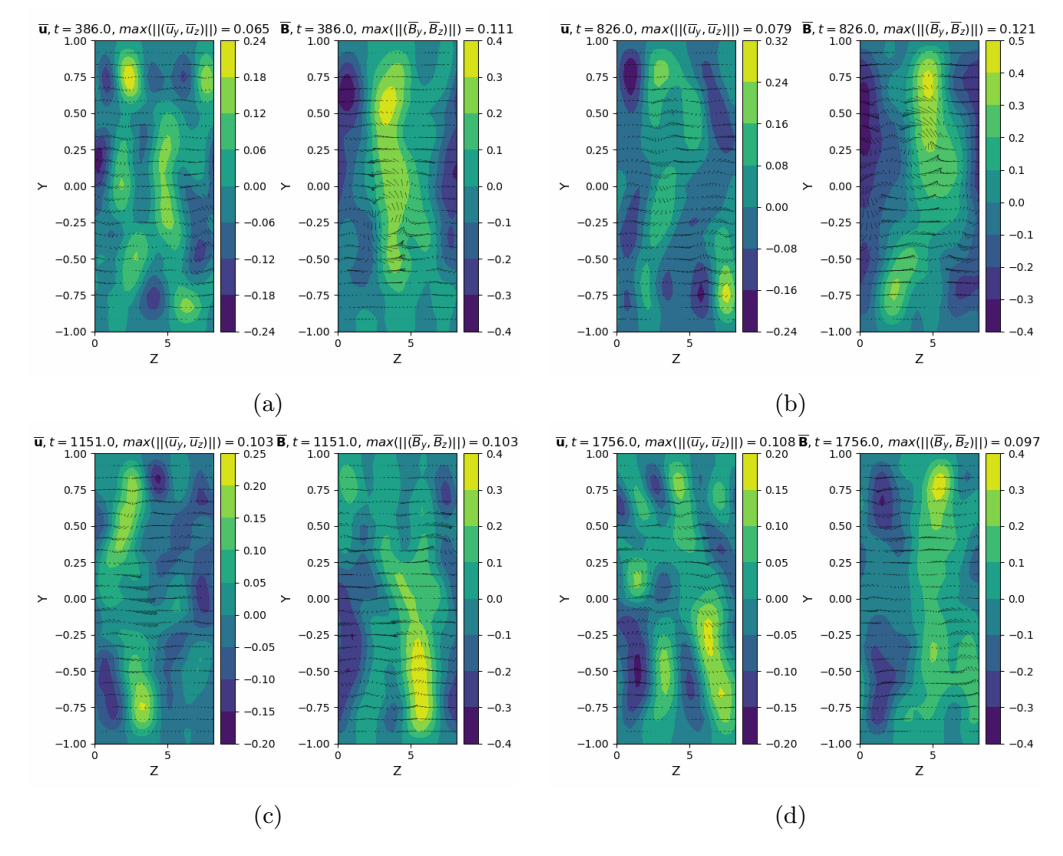


Figure 7: Snapshots of self sustaining turbulent equilibria maintaining finite amplitude components in both mean velocity \overline{u} and mean magnetic field \overline{B} . For each snapshot, on the left: streak velocity $\overline{u}_{xs} = \overline{u}_x - [\overline{u}_x]_z$ (contours) and roll velocity $(\overline{u}_y, \overline{u}_z)$ (vectors). On the right: streak magnetic field $\overline{B}_{xs} = \overline{B}_x - [\overline{B}_x]_z$ (contours) and roll magnetic field $(\overline{B}_y, \overline{B}_z)$ (vectors). Parameters: Re = 400, $Re_m = 600$, $\epsilon_{u'u'} = \epsilon_{B'B'} = 0$

$$I_D = sign(\overline{u}_{xs}) \cdot \left(\frac{\partial \overline{B'_x B'_y} - [\overline{B'_x B'_y}]_z}{\partial y} + \frac{\partial \overline{B'_x B'_z}}{\partial z}\right)$$
(8.5)

$$I_E = sign(\overline{u}_{xs}) \cdot (\frac{1}{Re} \Delta_1 \overline{u}_{xs})$$
(8.6)

The components of streak velocity forcing are identified as lift-up, (I_A) , Reynolds stress divergence, (I_B) , magnetic tension force due to mean magnetic field, (I_C) , divergence of fluctuation-fluctuation Maxwell stress anisotropic component, (I_D) , and viscous damping, (I_E) .

As example, we show the balance for our case of turbulence with Re = 400, $Re_m = 400$, $\epsilon_{\boldsymbol{u'u'}} = \epsilon_{\boldsymbol{B'B'}} = 3.9$. Temporal and spatial average diagnostics of I_A , I_B , I_C , I_D , I_E shown in figure 8 reveal that the lift-up process, I_A , alone contributes positively to streak maintenance while the Reynolds stress divergence, I_B , together with the fluctuation-fluctuation Maxwell stress anisotropic component divergence, I_D , contribute negatively to

streak velocity maintenance. Similar to the streak velocity force balance in wall bounded shear flow, the balance is between a positive contribution from lift-up, I_A , opposed by negative contributions from dissipation, I_E , and fluctuation-fluctuation stresses. The difference is that down gradient fluctuation-fluctuation stress divergence comes from not only Reynolds stress divergence, I_B , but also divergence of fluctuation-fluctuation Maxwell stress anisotropic component, I_D . The negative contributions of I_B and I_D indicate that both the fluctuation velocity field, u', and the fluctuation magnetic field, B', extract energy from the streak velocity, \bar{u}_{xs} .

We now consider the roll vorticity, $\overline{\omega}_{xr}$, maintenance using as a diagnostic the roll vorticity forcing. The roll vorticity forcing balance is:

$$\partial_{t}\overline{\omega}_{xr} = -((\overline{u_{y}}\partial_{y} + \overline{u_{z}}\partial_{z})\overline{\omega}_{x} - [(\overline{u_{y}}\partial_{y} + \overline{u_{z}}\partial_{z})\overline{\omega}_{x}]_{z}) + (\partial_{zz} - \partial_{yy})([u'_{y}u'_{z}]_{x} - [u'_{y}u'_{z}]_{x,z})$$

$$-\partial_{yz}([u'_{z}u'_{z}]_{x} - [u'_{y}u'_{y}]_{x}) + \Delta_{1}\frac{\overline{\omega}_{xr}}{Re} + (\partial_{yy} - \partial_{zz})\overline{B_{y}B_{z}} + \partial_{yz}(\overline{B_{z}B_{z}} - \overline{B_{y}B_{y}})$$

$$+(\partial_{yy} - \partial_{zz})\overline{B'_{y}B'_{z}} + \partial_{yz}(\overline{B'_{z}B'_{z}} - \overline{B'_{y}B'_{y}}).$$

$$(8.7)$$

As in the above case for the streak velocity maintenance dynamics, equations for the physically distinct terms in the dynamics maintaining $\overline{\omega}_{xr}$ are:

$$I_F = sign(\overline{\omega}_{xr}) \cdot \left(-(\overline{u_v}\partial_v + \overline{u_z}\partial_z)\overline{\omega}_x + [\overline{u_v}\partial_v + \overline{u_z}\partial_z)\overline{\omega}_x \right|_z)$$
(8.8)

$$I_G = sign(\overline{\omega}_{xr}) \cdot (\partial_{zz} - \partial_{yy})([u'_y u'_z]_x - [u'_y u'_z]_{x,z}) - \partial_{yz}([u'_z u'_z]_x - [u'_y u'_y]_x)$$
(8.9)

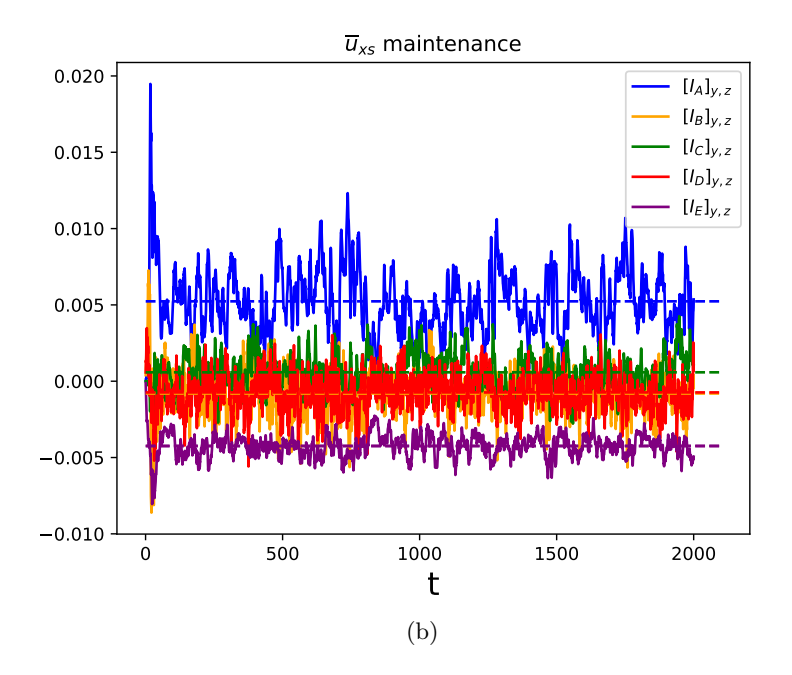
$$I_{H} = sign(\overline{\omega}_{xr}) \cdot ((\partial_{yy} - \partial_{zz})\overline{B_{y}B_{z}} + \partial_{yz}(\overline{B_{z}B_{z}} - \overline{B_{y}B_{y}}))$$
(8.10)

$$I_{I} = sign(\overline{\omega}_{xr}) \cdot ((\partial_{yy} - \partial_{zz})\overline{B'_{y}B'_{z}} + \partial_{yz}(\overline{B'_{z}B'_{z}} - \overline{B'_{y}B'_{y}}))$$
(8.11)

$$I_J = sign(\overline{\omega}_{xr}) \cdot \Delta_1 \frac{\overline{\omega}_{xr}}{Re}$$
(8.12)

The components of roll vorticity forcing are identified as advection by mean velocity, (I_F) , vorticity induced by Reynolds stress, (I_G) , vorticity induced by magnetic tension force of mean magnetic field, (I_H) , vorticity induced by fluctuation-fluctuation Maxwell stress anisotropic component, (I_I) , and dissipation, (I_J) . In wall bounded shear flow, the dominant balance maintaining the roll vorticity is between the positive contribution from Reynolds stress divergence, I_G , and the negative contribution from dissipation, I_J (Farrell et al. 2016). Temporal and spatial average diagnostics of I_F , I_G , I_H , I_I , I_J shown in figure 9 reveal that the Reynolds stress divergence term, I_G , and the fluctuation-fluctuation Maxwell stress anisotropic component divergence term, I_I , contribute positively to roll vorticity maintenance while the dissipation, I_J , contributes negatively. Similar to the roll vorticity force balance in wall bounded shear flow, the dominant balance is between the positive contributions from fluctuation-fluctuation terms opposed by a negative contribution from dissipation, I_J . The difference is that the positive contribution from the fluctuation-fluctuation terms come from not only the Reynolds stress term, I_H , but also the fluctuation-fluctuation Maxwell stress anisotropic component term, I_I .

These results show that the mechanisms maintaining \overline{u}_{xs} and $\overline{\omega}_{xr}$ in MHD turbulence are similar to those maintaining these components in wall-bounded shear flow, the main difference being the contribution by fluctuation-fluctuation Maxwell stress anistropic



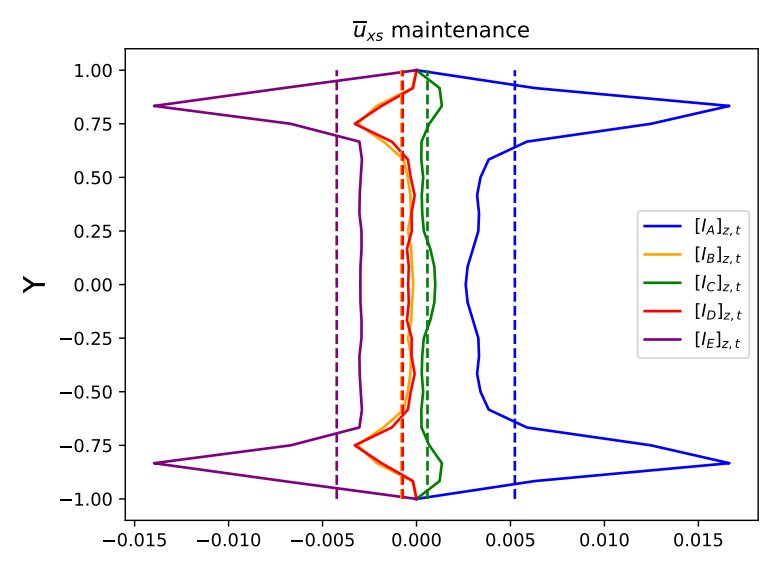
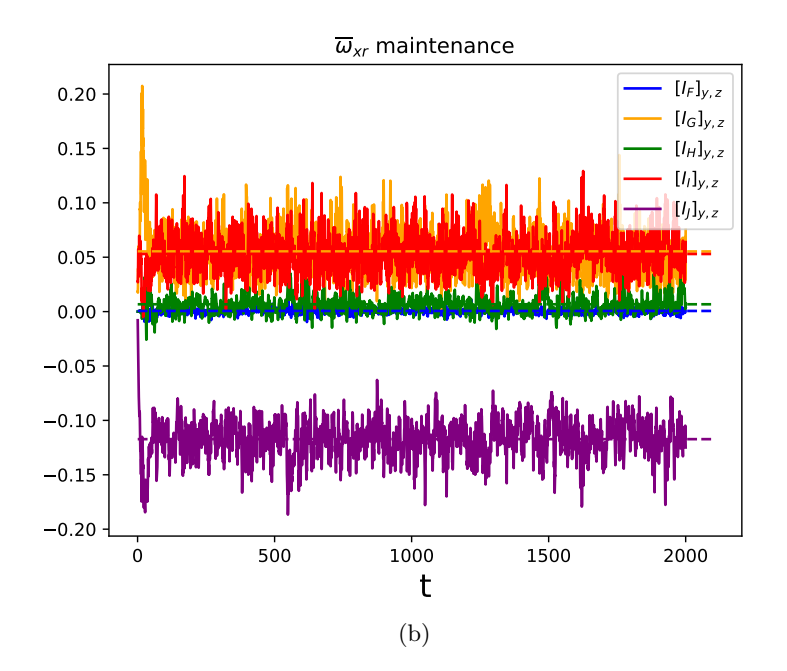


Figure 8: Equilibrium balance for the velocity streak, \overline{u}_{xs} , maintenance showing the lift-up term, $I_A(y,z,t)$, Reynolds stress divergence term, $I_B(y,z,t)$, magnetic tension force due to mean magnetic field $I_C(y,z,t)$, divergence of fluctuation-fluctuation Maxwell stress anisotropic component $I_D(y,z,t)$, and diffusion $I_E(y,z,t)$. Terms shown in (a) are averaged in both the spanwise direction, z, and the wall normal direction, y. Terms shown in (b) are averaged in the spanwise direction, z, and time t. Turbulence is at $R_e = 400$, $R_m = 400$, $\epsilon_{\boldsymbol{u}'\boldsymbol{u}'} = \epsilon_{\boldsymbol{B}'\boldsymbol{B}'} = 3.9$



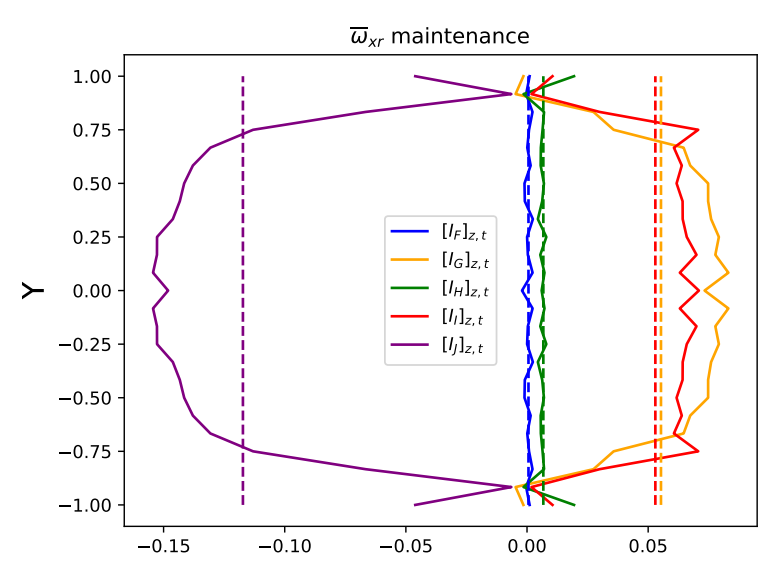


Figure 9: Equilibrium balance for streamwise vorticity (streamwise current density), $\overline{\omega}_{xr}$, containing mean advection term, $I_F(y,z,t)$, vorticity induced by Reynolds stress, $I_G(y,z,t)$, magnetic tension vorticity induced by mean magnetic field, $I_H(y,z,t)$, and vorticity induced by divergence of fluctuation-fluctuation Maxwell stress anistropic component, $I_I(y,z,t)$, and diffusion $I_J(y,z,t)$ (a) averaged in spanwise direction, z, and wall normal direction, y, (b) averaged in spanwise direction, z, and time, t. Turbulence is at $R_e = 400$, $R_m = 400$, $\epsilon_{u'u'} = \epsilon_{B'B'} = 3.9$.

component divergence contributing a negative forcing by I_D to \overline{u}_{xs} , indicative of transfer of streak energy to the fluctuation magnetic field, and a positive contribution by I_I to $\overline{\omega}_{xr}$, indicative of transfer of fluctuation magnetic energy to the roll circulation. These transfers are consistent with maintaining the velocity component in turbulent RSS.

9. Mechanisms maintaining the magnetic field in turbulent MHD RSS

We turn now to examine in a similar manner the physical mechanisms maintaining the magnetic field component of the RSS. The balance equation for maintenance of the streak magnetic field, $\overline{B}_{xs} = \overline{B_x} - [\overline{B_x}]_z$, is:

$$\partial_{t}\overline{B}_{xs} = (\partial_{y}\overline{u_{x}})\overline{B_{y}} + (\partial_{z}\overline{u_{x}})\overline{B_{z}} - [(\partial_{y}\overline{u_{x}})\overline{B_{y}} + (\partial_{z}\overline{u_{x}})\overline{B_{z}}]_{z}
+ (\overline{(\partial_{y}u'_{x})B'_{y}} + \overline{(\partial_{z}u'_{x})B'_{z}} - \overline{[(\partial_{y}u'_{x})B'_{y}} + \overline{(\partial_{z}u'_{x})B'_{z}}]_{z})
- ((\partial_{y}\overline{B_{x}})\overline{u_{y}} + ((\partial_{z}\overline{B_{x}})\overline{u_{z}}) - [(\partial_{y}\overline{B_{x}})\overline{u_{y}} + (\partial_{z}\overline{B_{x}})\overline{u_{z}}]_{z})
- (\overline{(\partial_{y}B'_{x})u'_{y}} + \overline{(\partial_{z}B'_{x})u'_{z}} - \overline{[(\partial_{y}B'_{x})u'_{y}} + \overline{(\partial_{z}B'_{x})u'_{z}}]_{z}) + \frac{1}{Re_{B}}\Delta_{1}\overline{B}_{xs}$$

$$(9.1)$$

As in the above case for the streak velocity maintenance dynamics, equations for the physically distinct terms in the dynamics maintaining the streak magnetic field \overline{B}_{xs} are:

$$I_{BA} = sign(\overline{B}_{xs}) \cdot ((\partial_u \overline{u_x}) \overline{B_y} + (\partial_z \overline{u_x}) \overline{B_z} - [(\partial_u \overline{u_x}) \overline{B_y} + (\partial_z \overline{u_x}) \overline{B_z}]_z)$$
(9.2)

$$I_{BB} = sign(\overline{B}_{xs}) \cdot (\overline{(\partial_y u_x') B_y'} + \overline{(\partial_z u_x') B_z'} - [\overline{(\partial_y u_x') B_y'} + \overline{(\partial_z u_x') B_z'}]_z)$$
(9.3)

$$I_{BC} = sign(\overline{B}_{xs}) \cdot \left(-((\partial_u \overline{B}_x) \overline{u}_y + (\partial_z \overline{B}_x) \overline{u}_z - [(\partial_u \overline{B}_x) \overline{u}_y + (\partial_z \overline{B}_x) \overline{u}_z]_z) \right) \tag{9.4}$$

$$I_{BD} = sign(\overline{B}_{xs}) \cdot \left(-(\overline{(\partial_y B_x') u_y'} + \overline{(\partial_z B_x') u_z'} - [\overline{(\partial_y B_x') u_y'} + \overline{(\partial_z B_x') u_z'}]_z) \right)$$
(9.5)

$$I_{BE} = sign(\overline{B}_{xs}) \cdot \frac{1}{Re_B} \Delta_1 \overline{B}_{xs} \tag{9.6}$$

The components of streak magnetic field forcing are identified as mean tilting, (I_{BA}) , fluctuation tiliting, (I_{BB}) , mean advection, (I_{BC}) , fluctuation advection, (I_{BD}) , and diffusive damping, (I_{BE}) . Temporal and spatial average diagnostics of I_{BA} , I_{BB} , I_{BC} , I_{BD} , and I_{BE} shown for our case of turbulence with Re = 400, $Re_m = 400$, $\epsilon_{u'u'} = \epsilon_{B'B'} = 3.9$ in figure 10 reveal that the mean tilting process, I_{BA} , alone contributes positively to the maintenance of the magnetic field of the streak, while the fluctuation tilting, I_{BB} , together with the fluctuation advection, I_{BD} , contribute negatively. In analogy with streak velocity maintenance, the balance is between the positive contribution from mean tilting, I_{BA} , opposed by negative contributions from dissipation, I_{BE} , and fluctuation-fluctuation terms. The main difference is streak velocity uses lift up, I_A , to produce the positive contribution whereas streak magnetic field uses mean tilting, I_{BA} , to produce the positive contribution. The negative contributions of fluctuation tilting, I_{BB} , and fluctuation advection, I_{BD} , indicate that the correlation between the fluctuation velocity field, u', and the fluctuation magnetic field, u', results in systematic extraction of energy

from the streak magnetic field, \overline{B}_{xs} , which energy is transferred to u' and B', consistent with the operation of an equivalent α effect.

We now form the curl of the magnetic field in the y-z plane, $\overline{\zeta_x} \equiv -\partial_z \overline{B_y} + \partial_y \overline{B_z}$, and take as our diagnostic for the roll magnetic field the quantity $\overline{\zeta_x}$ after removal of its spanwise average, $\overline{\zeta}_{xr} \equiv \overline{\zeta}_x - [\overline{\zeta}_x]_z$. The forcing of this quantity, which can be identified as the current density flowing into the y-z plane, has balance:

$$\partial_{t}\overline{\zeta}_{xr} = \partial_{y}((\partial_{y}\overline{u_{z}})\overline{B_{y}} + (\partial_{z}\overline{u_{z}})\overline{B_{z}}) - \partial_{z}((\partial_{y}\overline{u_{y}})\overline{B_{y}} + (\partial_{z}\overline{u_{y}})\overline{B_{z}})$$

$$-[\partial_{y}((\partial_{y}\overline{u_{z}})\overline{B_{y}} + (\partial_{z}\overline{u_{z}})\overline{B_{z}}) - \partial_{z}((\partial_{y}\overline{u_{y}})\overline{B_{y}} + (\partial_{z}\overline{u_{y}})\overline{B_{z}})]_{z}$$

$$+\partial_{y}((\overline{\partial_{y}u'_{z}})B'_{y} + (\overline{\partial_{z}u'_{z}})B'_{z}) - \partial_{z}((\overline{\partial_{y}u'_{y}})B'_{y} + (\overline{\partial_{z}u'_{y}})B'_{z})$$

$$-[\partial_{y}((\overline{\partial_{y}u'_{z}})B'_{y} + (\overline{\partial_{z}u'_{z}})B'_{z}) - \partial_{z}((\overline{\partial_{y}u'_{y}})B'_{y} + (\overline{\partial_{z}u'_{y}})B'_{z})]_{z}$$

$$+\partial_{z}((\partial_{y}\overline{B_{y}})\overline{u_{y}} + (\partial_{z}\overline{B_{y}})\overline{u_{z}}) - \partial_{y}((\partial_{y}\overline{B_{z}})\overline{u_{y}} + (\partial_{z}\overline{B_{z}})\overline{u_{z}})$$

$$-[\partial_{z}((\partial_{y}\overline{B_{y}})u'_{y} + (\partial_{z}\overline{B_{y}})u'_{z}) - \partial_{y}((\overline{\partial_{y}B'_{z}})u'_{y} + (\overline{\partial_{z}B_{z}})u'_{z})]_{z} +$$

$$+\partial_{z}((\overline{\partial_{y}B'_{y}})u'_{y} + (\overline{\partial_{z}B'_{y}})u'_{z}) - \partial_{y}((\overline{\partial_{y}B'_{z}})u'_{y} + (\overline{\partial_{z}B'_{z}})u'_{z})]_{z} +$$

$$-[\partial_{z}((\overline{\partial_{y}B'_{y}})u'_{y} + (\overline{\partial_{z}B'_{y}})u'_{z}) - \partial_{y}((\overline{\partial_{y}B'_{z}})u'_{z})]_{z} + \frac{1}{Re_{B}}\Delta_{1}\overline{\zeta}_{xr}$$

As in the above case for the streak magnetic field maintenance balance, equations for the physically distinct terms in the dynamics maintaining $\bar{\zeta}_{xr}$ are:

$$I_{BF} = sign(\overline{\zeta}_{xr}) \cdot (\partial_y((\partial_y \overline{u_z})\overline{B_y} + (\partial_z \overline{u_z})\overline{B_z}) - \partial_z((\partial_y \overline{u_y})\overline{B_y} + (\partial_z \overline{u_y})\overline{B_z}) - [\partial_y((\partial_y \overline{u_z})\overline{B_y} + (\partial_z \overline{u_z})\overline{B_z}) - \partial_z((\partial_y \overline{u_y})\overline{B_y} + (\partial_z \overline{u_y})\overline{B_z})]_z)$$

$$(9.8)$$

$$I_{BG} = sign(\overline{\zeta}_{xr}) \cdot (\partial_y(\overline{(\partial_y u_z')}B_y' + \overline{(\partial_z u_z')}B_z') - \partial_z(\overline{(\partial_y u_y')}B_y' + \overline{(\partial_z u_y')}B_z') - [\partial_y(\overline{(\partial_y u_z')}B_y' + \overline{(\partial_z u_z')}B_z') - \partial_z(\overline{(\partial_y u_y')}B_y' + \overline{(\partial_z u_y')}B_z')]_z)$$

$$(9.9)$$

$$I_{BH} = sign(\overline{\zeta}_{xr}) \cdot (\partial_z((\partial_y \overline{B_y})\overline{u_y} + (\partial_z \overline{B_y})\overline{u_z}) - \partial_y((\partial_y \overline{B_z})\overline{u_y} + (\partial_z \overline{B_z})\overline{u_z}) - [\partial_z((\partial_y \overline{B_y})\overline{u_y} + (\partial_z \overline{B_y})\overline{u_z}) - \partial_y((\partial_y \overline{B_z})\overline{u_y} + (\partial_z \overline{B_z})\overline{u_z})]_z)$$

$$(9.10)$$

$$I_{BI} = sign(\overline{\zeta}_{xr}) \cdot (\partial_z (\overline{(\partial_y B'_y) u'_y} + \overline{(\partial_z B'_y) u'_z}) - \partial_y (\overline{(\partial_y B'_z) u'_y} + \overline{(\partial_z B'_z) u'_z}) - [\partial_z (\overline{(\partial_y B'_y) u'_y} + \overline{(\partial_z B'_y) u'_z}) - \partial_y (\overline{(\partial_y B'_z) u'_y} + \overline{(\partial_z B'_z) u'_z})]_z)$$

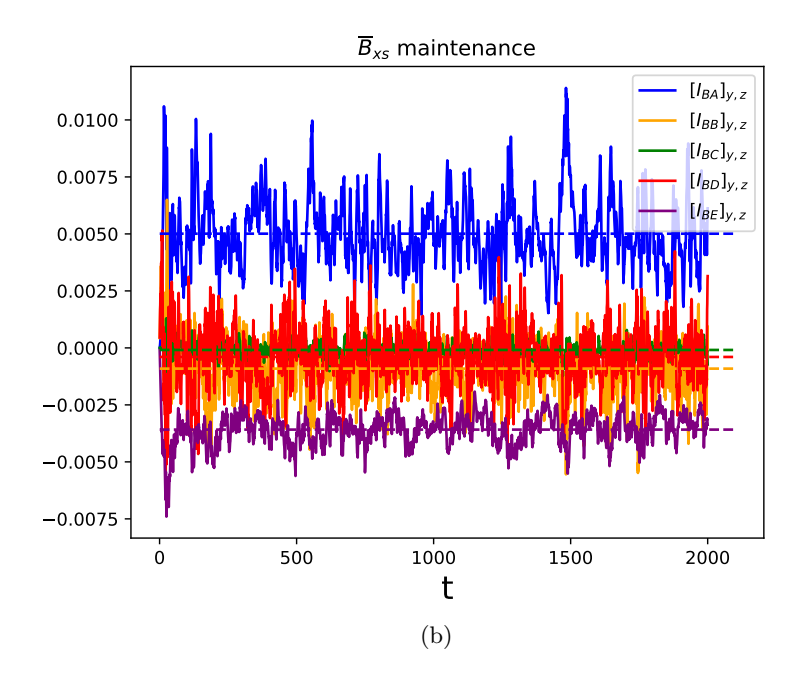
$$(9.11)$$

$$I_{BJ} = sign(\overline{\zeta}_{xr}) \cdot (\frac{1}{Re_B} \Delta_1 \overline{\zeta}_{xr})$$
(9.12)

These components of roll current density forcing are identified as the current density in the x direction induced by mean tilting and stretching, (I_{BF}) , fluctuation tilting and stretching, (I_{BG}) , mean advection, (I_{BH}) , fluctuation advection, (I_{BI}) , and dissipation, (I_{BJ}) .

Temporal and spatial average diagnostics of I_{BF} , I_{BG} , I_{BH} , I_{BI} , and I_{BJ} are shown in figure 11. These diagnostics reveal that both fluctuation tilting and stretching, I_{BG} , and fluctuation advection, I_{BI} , contribute positively to maintaining the current density of the roll while dissipation, I_{BJ} , contributes negatively.

We note that fluctuation tilting and stretching, I_{BG} , and fluctuation advection, I_{BI} are the fluctuation forcing for the roll magnetic field and therefore, together with the extraction of energy from the streak magnetic field, \overline{B}_{xs} , and transfer to u' and B' as



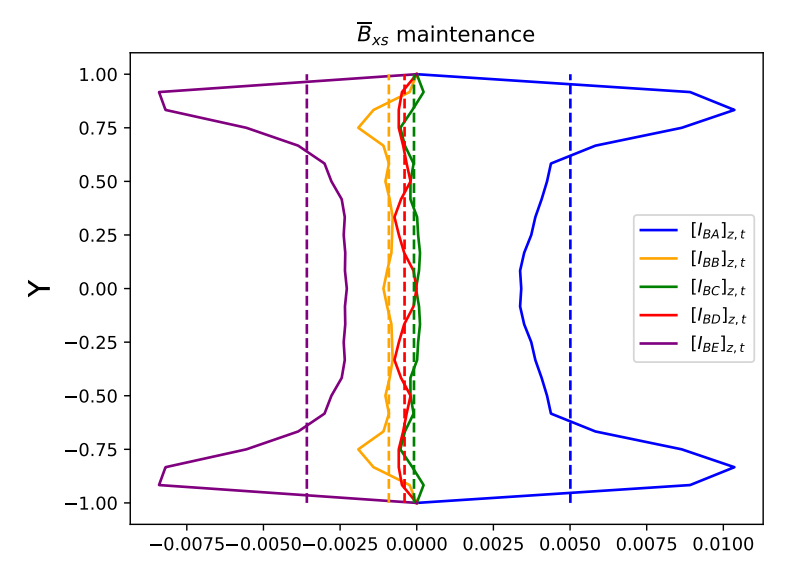


Figure 10: Equilibrium balance of magnetic field streak, B_{xs} , in RSS turbulence. Shown are mean field tilting, I_{BA} , fluctuation-fluctuation tilting, I_{BB} , mean field advection, I_{BC} , fluctuation-fluctuation advection, I_{BD} , and diffusion I_{BE} . (a) averaged in spanwise direction z and wall normal direction y (b) averaged in spanwise direction z and time t. Turbulence is at Re = 400, $Re_m = 400$, $\epsilon_{\boldsymbol{u'u'}} = \epsilon_{\boldsymbol{B'B'}} = 3.9$.

shown above in the balance maintaining streak magnetic field \overline{B}_{xs} , constitute the explicit expression of the α effect in this turbulent MHD RSS.

Comparing this roll current density force balance with the force balance of the roll vorticity shown above we note that in both cases the dominant balance is between the positive contributions from fluctuation-fluctuation terms opposed by a negative contribution from dissipation. Despite differences in physical interpretations of individual terms in these balances, our results show that the mechanisms maintaining the magnetic field components, \overline{B}_{xs} and $\overline{\zeta}_{xr}$, in turbulent MHD RSS are remarkably parallel to the mechanisms maintaining the velocity components, \overline{u}_{xs} and $\overline{\omega}_{xr}$.

Summarizing, the velocity streak is produced by lift up and the magnetic field streak is produced by tilting. Maintenance of both lift up and tilting require maintenance of the respective curl components $\overline{\omega}_{xr}$ and $\overline{\zeta}_{xr}$. These are both maintained against dissipation by positive contributions produced by fluctuation-fluctuation terms. We find two distinct fluctuation-fluctuation terms exist for each, I_G and I_I for $\overline{\omega}_{xr}$ maintenance and I_{BG} and I_{BI} for $\overline{\zeta}_{rr}$ maintenance.

The focus of the preceding and this section was on understanding maintenance of the components of the RSS contained in the mean velocity field \overline{u} and mean magnetic field \overline{B} . We next turn our attention to the dynamics of the fluctuation components contained in the covariance.

10. Maintenance of the fluctuation turbulent kinetic and magnetic energy components

Fluctuation turbulent kinetic energy (TKE) and turbulent magnetic energy (TME) are defined as:

$$TKE(t) = \frac{1}{2} [u_x'^2 + u_y'^2 + u_z'^2]_{x,y,z}$$
 (10.1)

$$TME(t) = \frac{1}{2} [B_x^{\prime 2} + B_y^{\prime 2} + B_z^{\prime 2}]_{x,y,z}$$
 (10.2)

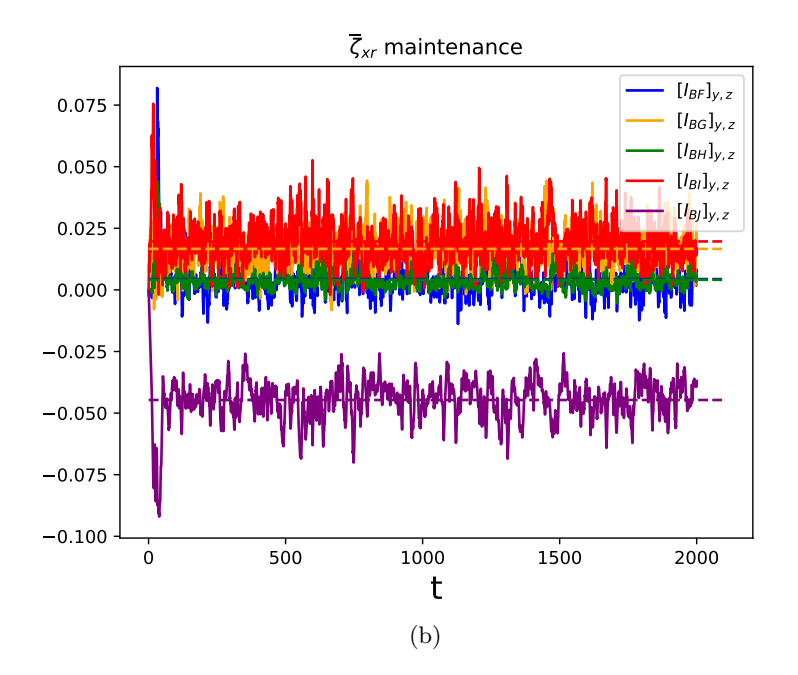
Equations for TKE and TME are:

$$\frac{\partial TKE}{\partial t} = -[\nabla \overline{\boldsymbol{u}} : \overline{\boldsymbol{u'} \otimes \boldsymbol{u'}}]_{y,z} + [\nabla \overline{\boldsymbol{B}} : \overline{\boldsymbol{u'} \otimes \boldsymbol{B'}}]_{y,z} - \frac{1}{Re} [\overline{\nabla \boldsymbol{u'} : \nabla \boldsymbol{u'}}]_{y,z}$$
(10.3)

$$\frac{\partial TME}{\partial t} = [\nabla \overline{\boldsymbol{u}} : \overline{\boldsymbol{B'} \otimes \boldsymbol{B'}}]_{y,z} - [\nabla \overline{\boldsymbol{B}} : \overline{\boldsymbol{B'} \otimes \boldsymbol{u'}}]_{y,z} - \frac{1}{Re_m} [\overline{\nabla \boldsymbol{B'}} : \overline{\nabla \boldsymbol{B'}}]_{y,z}$$
(10.4)

Mechanistic partition of the TKE and TME equations can be approximated schematically as:

$$\frac{\partial TKE}{\partial t} \approx \mathcal{P}_{\overline{u}_x \to TKE} + \mathcal{P}_{\overline{B}_x \to TKE} + \mathcal{E}_{TKE}$$
(10.5)



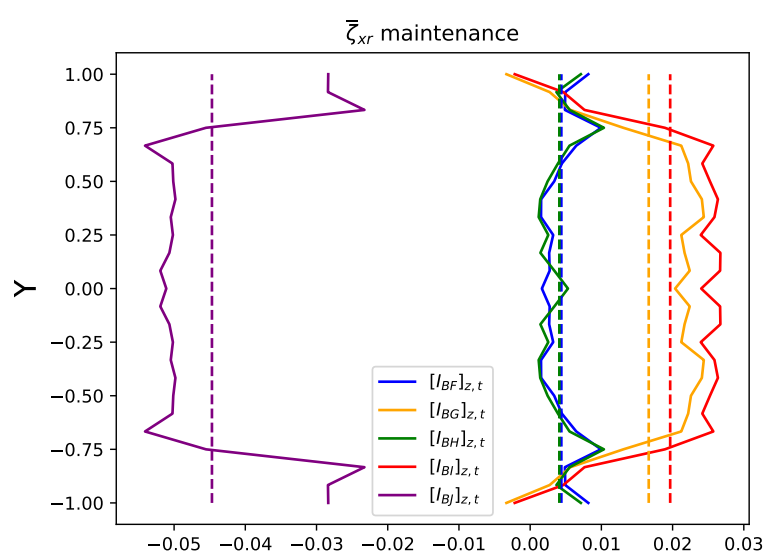


Figure 11: Equilibrium balance of magnetic field roll vorticity density in RSS turbulence. Shown are the mean tilting term, I_{BF} , fluctuation-fluctuation tilting, I_{BG} , mean advection of magnetic vorticity, I_{BH} , fluctuation-fluctuation advection, I_{BI} , and diffusion of magnetic field vorticity, I_{BJ} . (a) averaged in spanwise direction z and wall normal direction y (b) averaged in spanwise direction z and time t. Turbulence is at Re = 400, $Re_m = 400$, $\epsilon_{u'u'} = \epsilon_{B'B'} = 3.9$.

$$\frac{\partial TME}{\partial t} \approx \mathcal{P}_{\overline{u}_x \to TME} + \mathcal{P}_{\overline{B}_x \to TME} + \mathcal{E}_{TME}$$
 (10.6)

23

in which these separate mechanisms have been identified:

$$\mathcal{P}_{\overline{u}_x \to TKE} = -\left[\frac{\partial \overline{u_x}}{\partial y} \overline{u_y' u_x'}\right]_{y,z} - \left[\frac{\partial \overline{u_x}}{\partial z} \overline{u_z' u_x'}\right]_{y,z}$$
(10.7)

$$\mathcal{P}_{\overline{B}_x \to TKE} = \left[\frac{\partial \overline{B_x}}{\partial y} \overline{B_y' u_x'} \right]_{y,z} + \left[\frac{\partial \overline{B_x}}{\partial z} \overline{B_z' u_x'} \right]_{y,z}$$
(10.8)

$$\mathcal{P}_{\overline{u}_x \to TME} = \left[\frac{\partial \overline{u}_x}{\partial y} \overline{B'_y B'_x}\right]_{y,z} + \left[\frac{\partial \overline{u}_x}{\partial z} \overline{B'_z B'_x}\right]_{y,z}$$
(10.9)

$$\mathcal{P}_{\overline{B}_x \to TME} = -\left[\frac{\partial \overline{B_x}}{\partial y} \overline{u_y' B_x'}\right]_{y,z} - \left[\frac{\partial \overline{B_x}}{\partial z} \overline{u_z' B_x'}\right]_{y,z}$$
(10.10)

$$\mathcal{E}_{TKE} = -\frac{1}{Re} [\overline{\nabla u'} : \overline{\nabla u'}]_{y,z}$$
 (10.11)

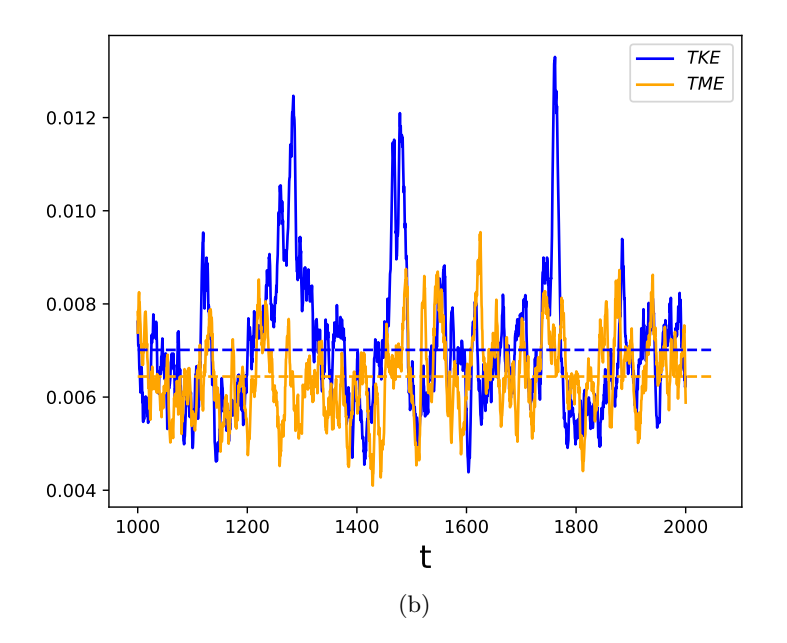
$$\mathcal{E}_{TME} = -\frac{1}{Re_m} [\overline{\nabla \mathbf{B'}} : \overline{\nabla \mathbf{B'}}]_{y,z}. \tag{10.12}$$

These terms are the TKE production due to fluctuation-fluctuation momentum flux, $\mathcal{P}_{\overline{u}_x \to TKE}$, TKE production due to fluctuation-fluctuation magnetic field flux, $\mathcal{P}_{\overline{B}_x \to TKE}$, and dissipation due to viscosity, \mathcal{E}_{TKE} . Similarly, terms associated with dynamics of TME are TME production due to the Maxwell stress anisotropic component, $\mathcal{P}_{\overline{u}_x \to TME}$, TME production due to fluctuation-fluctuation magnetic field flux, $\mathcal{P}_{\overline{B}_x \to TME}$, and dissipation due to magnetic diffusivity, \mathcal{E}_{TME} .

Shown in panel (a) of figure 12 is a time series of both the TKE and TME for our case of turbulence at Re = 400, $Re_m = 400$, $\epsilon_{u'u'} = \epsilon_{B'B'} = 3.9$. In panel (b) is shown time series of the associated terms in the energy balance. Both the TKE and TME extract energy from the mean streamwise velocity $\overline{u_x}$ and mean magnetic field $\overline{B_x}$. These positive contributions are primarily balanced by dissipation.

11. Discussion and Conclusion

The MHD equations of Couette flow formulated as a perturbation stability problem about a laminar velocity state do not support instability, much less an unstable RSS with large scale coherent velocity and magnetic fields. Although the RSS is ubiquitous in both turbulent and transitional shear flows and DNS experiments confirmed that it is required for maintaining turbulence in shear flow, the existence of an instability with RSS form and a dynamical system in which this structure maintaines a statistically stable turbulent state in the NS eluded explicit dynamical analysis in both conducting and nonconducting shear flow. The reason why the dynamics of the RSS remained obscure is that this structure and the instability forming it are nonlinear. The key to discovering this foundational instability, and the pivotal dynamics of the RSS in general, lies in analyzing the turbulence dynamics using an SSD formulation of the NS. In the S3T SSD closed at second order the second cumulant, which is the ensemble mean covariance of the state fluctuations, is treated as a linear variable in the perturbation analysis, although it is quadratically nonlinear as a state variable, which allows the full power of linear perturbation analysis to be brought to bear on this nonlinear instability.



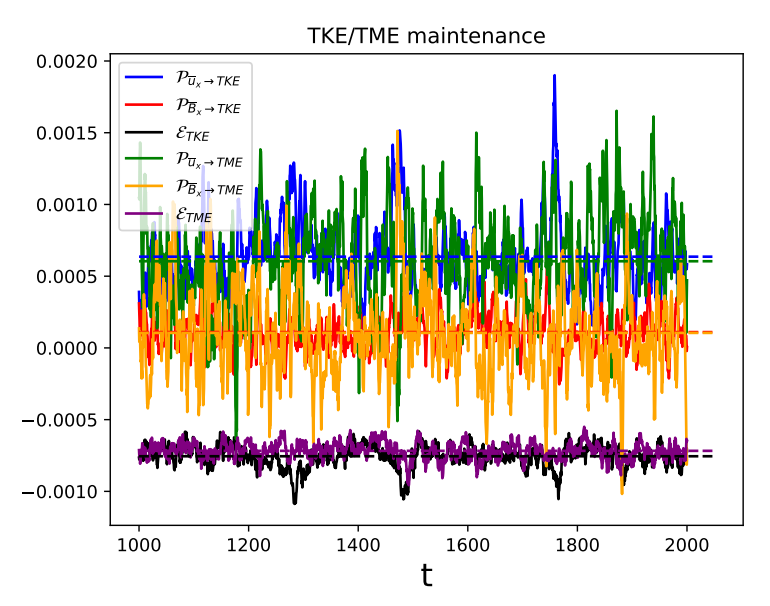


Figure 12: (a) Time series of TKE and TME (b) maintenance of TKE and TME. TKE production due to fluctuation-fluctuation momentum flux, $\mathcal{P}_{\overline{u}_x \to TKE}$, TKE production due to fluctuation-fluctuation magnetic field flux, $\mathcal{P}_{\overline{B}_x \to TKE}$, dissipation, \mathcal{E}_{TKE} . TME production due to the Maxwell stress anisotropic component, $\mathcal{P}_{\overline{u}_x \to TME}$, TME production due to fluctuation-fluctuation magnetic field flux, $\mathcal{P}_{\overline{B}_x \to TME}$, and dissipation, \mathcal{E}_{TME} . Turbulence is at Re = 400, $Re_m = 400$, $\epsilon_{\boldsymbol{u'u'}} = \epsilon_{\boldsymbol{B'B'}} = 3.9$.

Previously, SSD had been used to study the formation of the RSS as an unstable mode and its maintenance as a stable fixed point as well as the equilibration of the RSS to self-sustaining turbulent states in nonconducting wall bounded shear flow (Farrell et al. 2017; Farrell & Ioannou 2012). The similarity of the NS and induction equations motivated the extension of these previous results to the study of MHD turbulence in conducting Couette flow using SSD. Further motivation came from the fact that the RSS in shear flow supports a poloidal velocity field with a helical structure that suggests a natural support for maintaining an associated toroidal magnetic field. In this work we found that, in the presence of a background field of small amplitude random turbulence in a conducting Couette flow, RSS emerge as unstable modes with remarkably similar structure in the velocity field and the magnetic field - almost as if these two RSS coexisted with a 90° phase shift separating them in z. Moreover, we found that these RSS structures are synergistic in the sense of cooperating in the formation and growth of the instability although the ultimate energy source for the RSS is the velocity shear at the boundary. Because the SSD we use is the NS equations closed at second order, it contains the nonlinear mechanism responsible for establishing finite amplitude equilibrium states, both for fixed points and, in the case of turbulent RSS states, the statistical mean state. We identified equilibrium regimes consisting of stable, \overline{u} only RSS fixed points, stable $(\overline{u} \text{ and } B)$ fixed points containing both fields at finite amplitude, excited turbulent states, self sustaining turbulent states supporting \overline{u} only, and self sustaining turbulent states containing both (\overline{u} and B). These self sustaining states emerge after transition to RSS turbulence has occurred. They are revealed by eliminating the stochastic turbulence excitation from the SSD. If, when this is done, the turbulence transitions to a statistically stable turbulent state, we conclude that a self sustaining state is supported for the parameters used.

In both the fixed point and self sustaining states, maintenance of a coherent large scale RSS supporting only a mean \overline{u} field occurs for some parameters. For other parameters both the \overline{u} and \overline{B} field are supported in the RSS, which corresponds to a dynamo. Using the magnetic Prandtl number, Pr_m , as a parameter we found that transition from a self sustaining state in the velocity field only to a self sustaining state in both the velocity and the magnetic field, corresponding to a dynamo, manifested as an abrupt bifurcation in the statistical state occurring at a critical Pr_m .

Using the S3T SSD we are able to obtain and analyze the unstable RSS modes and the nonlinear equilibria proceeding from these modes, both fixed point and turbulent. This allowed us to study in detail the physical mechanisms underlying the RSS dynamics.

We found that the mechanism supporting the streak and the roll component of the velocity field of the turbulent MHD RSS is similar to that previously found to support the streak and the roll velocity component of the RSS in the SSD for non-conducting Couette flow. Dominant balance for the streak velocity in both case is between positive contributions from lift-up and negative contributions from dissipation and fluctuation-fluctuation terms. In turbulent MHD RSS, the difference is small fluctuation-fluctuation Maxwell stress components contributes additional negative forcing to maintaining \overline{u}_{xs} .

Similar to the roll vorticity force balance in nonconducting wall bounded shear flow, the dominant balance supporting the roll velocity component of the MHD RSS is between positive contributions from fluctuation-fluctuation terms opposed by a negative contribution from dissipation. In turbulent MHD RSS, the difference is that the positive contributions from the fluctuation-fluctuation terms come from not only the Reynolds stress term, but also the fluctuation-fluctuation Maxwell stress anisotropic component term which is indicative of a synergy between the velocity and magnetic field components in maintaining the combined RSS.

In the case of the magnetic field streak component of the RSS, \overline{B}_{xs} , we found that the dominant balance is between a positive contribution from mean tilting (which is analogous to lift-up in the maintenance of the streak velocity component), opposed by negative contributions from dissipation and fluctuation-fluctuation terms. The correlation between the fluctuation velocity field and the fluctuation magnetic field results in systematic extraction of energy from the streak magnetic field, which energy is transferred to the fluctuations.

Turning to the maintenance of the roll magnetic field component, which is the current density in the x direction, we find that fluctuation tilting and stretching, and fluctuation advection, contribute positively to maintaining the current density of the roll while dissipation, contributes negatively. In summary, in both the maintenance of the streak velocity and the streak magnetic field, fluctuation-fluctuation terms contribute negatively. Similarly, in both the maintenance of the roll velocity and the roll magnetic field, it is the fluctuation-fluctuation terms that contribute positively. This result demonstrates the centrality of fluxes arising from the correlation of turbulent fluctuations in the velocity and magnetic field in sustaining both the roll velocity and the roll (or poloidal) magnetic field that constitutes the α effect in maintaining the dynamo.

REFERENCES

- Butler, K. M. & Farrell, B. F. 1992 Three-dimensional optimal perturbations in viscous shear flows. *Phys. Fluids* 4, 1637–1650.
- ELLINGSEN T. & PALM E. 1975 Stability of linear flow. Physics of Fluids 18 487-488
- FARRELL, B. F. & IOANNOU, P. J. 1993 Optimal excitation of three-dimensional perturbations in viscous constant shear flow. *Phys. Fluids A* 5, 1390–1400.
- FARRELL B.F. & IOANNOU P.J. 1996a Generalized Stability Theory. Part I: Autonomous Operators. *Journal of the Atmospheric Sciences* **53** (14) 2025-2040
- FARRELL B.F. & IOANNOU P.J. 1996b Generalized Stability Theory. Part II: Nonautonomous Operators. *Journal of the Atmospheric Sciences* **53** (14) 2041-2053
- FARRELL B.F. & IOANNOU P.J. 1999a Ooptimal excitation of magnetic fields. *The. Astrophysical. Journal* **522** 1079-1087
- FARRELL B.F. & IOANNOU P.J. 1999b Stochastic dynamics of field generation in conducting fluids. The. Astrophysical. Journal **522** 1088-1099
- FARRELL, B. F. & IOANNOU, P. J. 2009b A stochastic structural stability theory model of the drift wave-zonal flow system. *Phys. Plasmas* 16, 112903.
- FARRELL, B. F. & IOANNOU, P. J. 2012 Dynamics of streamwise rolls and streaks in turbulent wall-bounded shear flow. *J. Fluid Mech.* **708**, 149–196.
- Farrell, B. F. & Ioannou, P. J. 2016 Structure and mechanism in a second-order statistical state dynamics model of self-sustaining turbulence in plane Couette flow. *Phys. Rev. Fluids* (submitted, arXiv:1607.05020).
- FARRELL, B. F., IOANNOU, P. J. & M.-A., NIKOLAIDIS 2017 Instability of the roll/streak structure induced by free-stream turbulence in pre-transitional Couette flow. *Phys. Rev. Fluids* (submitted, arXiv:1607.05018).
- Farrell B. F., Ioannou P. J., Jimenez J., Constantinou N. C., Lozano-Duran A. & Nikolaidis M. A. 2016 A statistical state dynamics-based study of the structure and mechanism of large-scale motions in plane Poiseuille flow. *J. Fluid Mechanics* **809** 290-315
- FARRELL, B. IOANNOU, P 2019 Statistical State Dynamics: A New Perspective on Turbulence in Shear Flow. Zonal Jets Phenomenology, Genesis, and Physics. Ed. Boris Galpirin and Peter L. Read. Cambridge University Press 2019.. 380-400.
- FARRELL B. F., IOANNOU P. J. & NIKOLAIDIS M. A. 2022 Mechanism of Roll-Streak Structure Formation and Maintenance in Turbulent Shear Flow. arXiv:2205.07469.
- Gustavsson L.H. 1991 Energy growth of three-dimensional disturbances in plane Poiseuille flow. *Journal of Fluid Mechanics* **224** 241–260.

- KIM E. & FARRELL B.F. 2025 Statistical State Dynamics based study of Langmuir Turbulence. arXiv:2509.00234
- KLINE S., REYNOLDS W.C., SCHRAUB F.A.& RUNSTADLER P.W. 1999 The structure of turbulent boundary layers. . J. Fluid. Mech 30 741-773.
- NIKOLAIDIS M. A., IOANNOU P. J. & FARRELL B. F. 2024 Fluctuation covariance-based study of roll-streak dynamics in Poiseuille flow turbulence. *J. Fluid Mechanics* **988** A14.
- REDDY S.C. & HENNINGSON D.S. 1993 Energy growth in viscous channel flows. *Journal of Fluid Mechanics* **252** 209-238
- Schmid, P. J. & Henningson, D. S. 2001 Stability and Transition in Shear Flows. Springer, New York.
- SMITH C.R. & METZLER S.P. 1983 The characteristics of low-speed streaks in the near-wall region of a turbulent boundary layer. J. Fluid. Mech 129 27-54